6-2020

Development of Catalytic Chromia-based Aerogels

Fiona Fitzgerald
Union College - Schenectady, NY

Development of Catalytic Chromia-based Aerogels

By

Fiona T. Fitzgerald

****

Submitted in partial fulfillment
of the requirements for
Honors in the Department of Biochemistry

UNION COLLEGE

June, 2020

ABSTRACT

FITZGERALD, FIONA Development of catalytic chromia-based aerogels. Department of Biochemistry. June 2020

Advisor: Mary K. Carroll

Over one billion automobiles are in use around the world, the majority of which employ internal combustion engines. Catalytic converters are used to convert the toxic compounds found in car exhaust -- carbon monoxide, nitrogen oxides (NOx) and hydrocarbons -- to less harmful gases. The typical catalytic converter employs as catalysts expensive raw materials (platinum, palladium and/or rhodium) wash-coated onto an alumina-based ceramic substrate. Aerogel materials have high surface area and thermal stability, properties that make them attractive for catalysis applications. Aerogels made with transition metal oxides are candidates to replace platinum in the catalytic converter. Chromium oxide (chromia) materials have demonstrated catalytic activity in other applications due to favorable redox chemistry, stability and selectivity. In this work, sol-gel synthesis techniques are adapted to a patented rapid supercritical extraction (RSCE) method to fabricate chromia and chromia-based catalytic aerogels. In one example of a co-precursor technique, a mixture (1:5 mole ratio) of chromium(III) to aluminum salt in ethanol is reacted with a weak base or proton scavenger to induce gelation. Following solvent exchanges of the wet gels with absolute ethanol, and RSCE processing yields chromia-alumina aerogels. Observed shrinkage is higher than for copper-containing aerogels fabricated via the same process. Physical characterization via several methods, including XRD and SEM, reveals post-calcination chromia-alumina aerogels contain α- Cr_2O_3 nanocrystals within the alumina backbone. Catalytic testing is evaluated using an in-house-constructed testbed in which the aerogel materials are

exposed to simulated automotive exhaust under temperature conditions that approximate those experienced in a catalytic converter. Chromia-alumina aerogels completely convert HC and CO gases at 400 °C under high air conditions and completely convert NO at 450 °C under low air conditions.

ACKNOWLEDGEMENTS

I would like to thank Professor Mary Carroll for her guidance and support throughout my investigations and experiments and also the writing of this thesis. I would also like to thank Professor Ann Anderson and Professor Brad Bruno for their assistance and guidance during this research project. Without the knowledge and dedicated assistance from these professors the outcomes of this project would not have been possible.

I would like to thank my peers in the Aerogel Laboratory for their thoughtful collaboration and assistance; especially: Diana Lang (BET/BJH analyses, 4g CuAl aerogel preparation, UCAT testing), Chris Avanessian (SEM/EDS imaging), Tommy Andre (XRD assistance); Bassem Darwish, Avi Gajjar and Margeaux Capron (fabrication assistance); Ryan Puglisi, Chris O'Brien and Matt LaRosa (UCAT testing).

I would also like to thank Union College, for funding through the Student Research Grants. This material is based upon work supported by the National Science Foundation under Grants No. NSF MRI CBET-1228851, NSF DMR-1828144 & NSF IIP-1918217.

TABLE OF CONTENTS

TABLE OF FIGURES

TABLE OF TABLES

1. INTRODUCTION

Aerogels

An aerogel can be characterized as a low density, highly porous and thermally stable amorphous nanoparticle structure. Aerogels are highly mesoporous particles and have an average pore diameter of 20 to 40 nm [1]. Aerogels can be produced by fabricating a sol-gel network from salt precursors and an epoxide assisted ring opener. The size and diameter of pores can be controlled through the sol-gel fabrication techniques and conditions; for example, by changing the rate of the hydrolysis reaction or the aging time. Solvent exchanges are performed using a variety of alcohols to wash out excess reagents and byproducts from the pores of the wet gels. In some cases leaching occurs, which refers to the loss of the aerogel base or co-precursor compound as waste from the pores. Aging is further important to strengthen the sol-gel network structure and integrity and, over time, changes the density of the nanomaterial, which helps strengthen the structure and reduce risk of fracture during drying via ambient pressure drying as presented in Figure 1-1 [2].

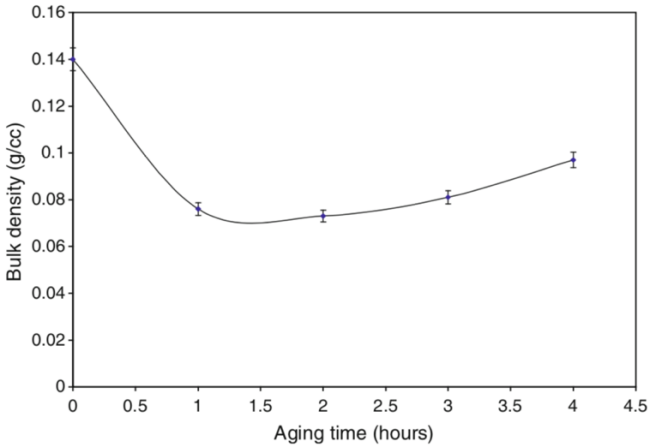

Figure 1-1: Relationship between aging and bulk density of aerogels [2].
*Reprinted by permission from **Springer Nature Customer Service Centre GmbH**: Springer*. Aerogels Handbook, *"Sodium Silicate Based Aerogels via Ambient Pressure Drying." Venkateswara Rao, A.; Pajonk, G. M.; Bangi, Uzma K. H.; Parvathy Rao, A., Koebel, M. M. © Springer Science + Business Media, LLC 2011 DOI 10.1007/978-1-4419-7589-8*.

Aerogels were first synthesized from silica, using sodium silicate salt (Na_2SiO_3) in 1932, but since the first synthesis aerogels have been produced from a number of other salts. For example, a very common aerogel backbone besides silica is alumina; however, alumina is known to be mechanically weak compared to silica and alumina gels fracture much easier than silica monoliths [3].

Today, many other precursors are used to produce silica aerogels in addition to sodium silicate salt (Na_2SiO_3), such as alkoxides: tetramethyl orthosilicate (TMOS) and tetraethyl orthosilicate (TEOS) to induce polymerization via hydrolysis reactions. The polymerization results in a silica matrix of siloxane groups (Si-O-Si); then a proton scavenger, such as propylene oxide or weak base can be used to pick up the H^+ ions in solution [4]. If propylene oxide is used, protonated propylene oxide undergoes an epoxide ring opening reaction induced by a nucleophile in the solution such as water. This is important to inhibit the formation of the hydroxo-aquo cation, and allows for formation of the sol-gel complex [5].

Similarly, high-surface-area alumina aerogels can be produced via alumina precursors such as aluminum isopropoxide, aluminum *sec*-butoxide or aluminum chloride hexahydrate ($AlCl_3 \cdot 6H_2O$) and an alkoxide, such as ethanol [6]. Sol-gel formation of the polymerized alumina lattice can then be induced using propylene oxide as explained above. After sufficient drying aerogels can be characterized to understand the electronic structure and phases of elements present, such as alumina, the aerogel backbone of the aerogels studied in this thesis. Alumina has multiple transition states from $\gamma \rightarrow \delta \rightarrow \theta \rightarrow \alpha$, in which α is the most stable form of Al_2O_3 and forms an octahedral lattice in which ⅔ of the structure is due to a cationic hexagonal sublattice [7]. α-alumina is commonly known as corundum and is the predominant phase of alumina seen in alumina-based aerogels [8,9,10].

Aerogels are very diverse nanomaterials due to the fact that many different elements and particles can be incorporated in them to change their physical characteristics, color, mesoporous structure and catalytic abilities. This thesis will focus on incorporating transition metal oxides (TMOs) into aerogels to give them catalytic characteristics. Transition metal oxides are oxidative catalysts due to the oxygen atom bound to one of the various transition metals. TMOs have half-filled d orbitals which allow them to exist in multiple transition states, which accounts for the higher activity, sensitivity to deactivation and overall catalytic abilities of TMOs [11, 12]. There are two common methods to incorporate TMOs within alumina aerogels: co-precursor techniques or impregnation techniques. Co-precursor techniques call for a mixture of a salt containing the transition metal, an aluminum salt and an alcohol, this solution undergoes hydrolysis and condensation reactions driven by the addition of an epoxide acid

scavenger. As the epoxide acid scavenger is protonated the pH of the solution gradually rises and induces sol-gel formation of the transition metal oxide network within the sol-gel matrix [13]. In contrast, impregnation techniques are employed when performing solvent exchanges on alumina (or silica) wet gels. Instead of solely using an alcohol for the first of three solvent exchanges; a salt containing the transition metal is dissolved in the alcohol and this solution is used for the solvent exchange. The TMO covalently bonds to the mesoporous wet gel and is now incorporated into the aerogel via covalent interactions [6].

At this stage wet gels have been produced but to initiate the transition to an aerogel a drying technique must be used to replace the liquid in the pores with air without affecting the porous structure or collapsing the gel network. The most commonly used drying techniques to maintain the integrity of the porous structure and gel network are based on supercritical extraction [3]. The supercritical point of a solvent can be achieved by using a temperature and pressure ramp to vent off bulk fluid above the critical temperature and pressure [14]. Union College has a patented rapid supercritical extraction (RSCE) technique utilizing a stainless-steel metal mold, high temperature gaskets and a hydraulic hot press (US Patents 7,384,988 and 8,080,591). The hydraulic hot press seals the mold due to the restraining force and heats the mold. After the supercritical point of the solvent in the wet gel has been exceeded, the hydraulic hot press releases the supercritical fluid while cooling the mold at a controlled rate, resulting in the aerogel [15]. A disadvantage of supercritical drying is the possibility of shrinkage due to collapse of the pores as the fluid is exchanged for gas. Shrinkage is caused by intense capillary forces and stress during evaporative or supercritical drying inside the wet gel matrix

which overall can lead to a 30% decrease in aerogel volume compared to the initial wet gel volume [3, 12]. However, the Union College RSCE technique mitigates shrinkage during supercritical extraction through the gradual temperature and pressure ramp until the supercritical point of the solvent is met. Further, the hot press is held at the highest temperature and pressure for 30 minutes to allow thermal equilibrium to be met. The gradual decrease in temperature and pressure to release the constraint on mold maintains the aerogel network without putting excessive force on the aerogel or changing the size [15].

Catalytic abilities of aerogels have been significantly researched over the past twenty years and progress has been made to determine if additional elements can enhance the catalytic ability of silica or alumina-based aerogels. Davood Karami published a review of the catalytic applications of aerogels in 2018 [16]. He stated that among the many viable aerogel applications, the ability to convert CO and propane is a promising application due to the ideal physicochemical properties, extensive research and recent advancements in production and cost reduction [16]. Many commercial catalysts utilize noble metals or TMOs to produce catalytic effects. It has been found that noble metals such as Pt, Pd, Ru, Rh, and Ir are the most active and tolerant to poisons. However, these metals are very expensive, and usage of noble metals significantly affects the environment, through mining for noble metals. The Wall Street Journal published an article in January of 2020 stating that recent, stricter, emission laws have caused automobile manufacturers to utilize more rhodium (Rh) in catalytic converter production. However, since rhodium is mined as a byproduct of gold, platinum and palladium, it has no futures market which makes the price more volatile. The sudden increase in the

demand for rhodium in conjunction with the increasing price of palladium cost the automobile industry $8 billion in metals alone during the month of January [17].

The most active TMOs are Cobalt (Co), Chromium (Cr), Copper (Cu), Manganese (Mn), and Vanadium (V) due to their ability to fully oxidize; however, these are less active than noble metals [18]. TMO catalytic aerogels have been successfully synthesized and characterized in the Union College Aerogel Laboratory incorporating copper (Cu), cobalt (Co), cerium (Ce), nickel (Ni) or vanadium (V) into both silica- and/or alumina-based aerogels using the impregnation technique and, in some cases, co-precursor technique [4, 8, 19, 20, 21]. These transition metals were chosen due to their ability to rapidly change between oxidation states, which makes them possible oxygen storage units in catalysts, such as catalytic converters [6].

Catalytic Converters

A catalytic converter is a three-way catalyst (TWC) and makes up a portion of an automotive exhaust system. A TWC mitigates automotive pollution that results due to incomplete combustion of gasoline. Hydrocarbon fuels are mostly or partially burnt and result in by products of hydrocarbons and carbon monoxide; while high temperature flame combustion causes nitrogen and oxygen to combine to form nitric oxide. Platinum group elements (PGE) are the predominant TWCs utilized to reduce nitrogen oxides (NOx), carbon monoxide (CO) and hydrocarbons (HC), due to their high activity as explained earlier. However, since catalytic converters were created almost 50 years ago to control tailpipe pollutants, a need for a substitute had been eminent [22]. Life cycle assessments of catalytic converters have been performed to determine their benefits, environmental impact and if the local reduction of automotive emissions due to TWC

outweighs the increasing global impact of mining of precious PGE [23]. A schematic of the gas flow and reaction processes through a TWC catalytic converter can be seen in Figure 1-2.

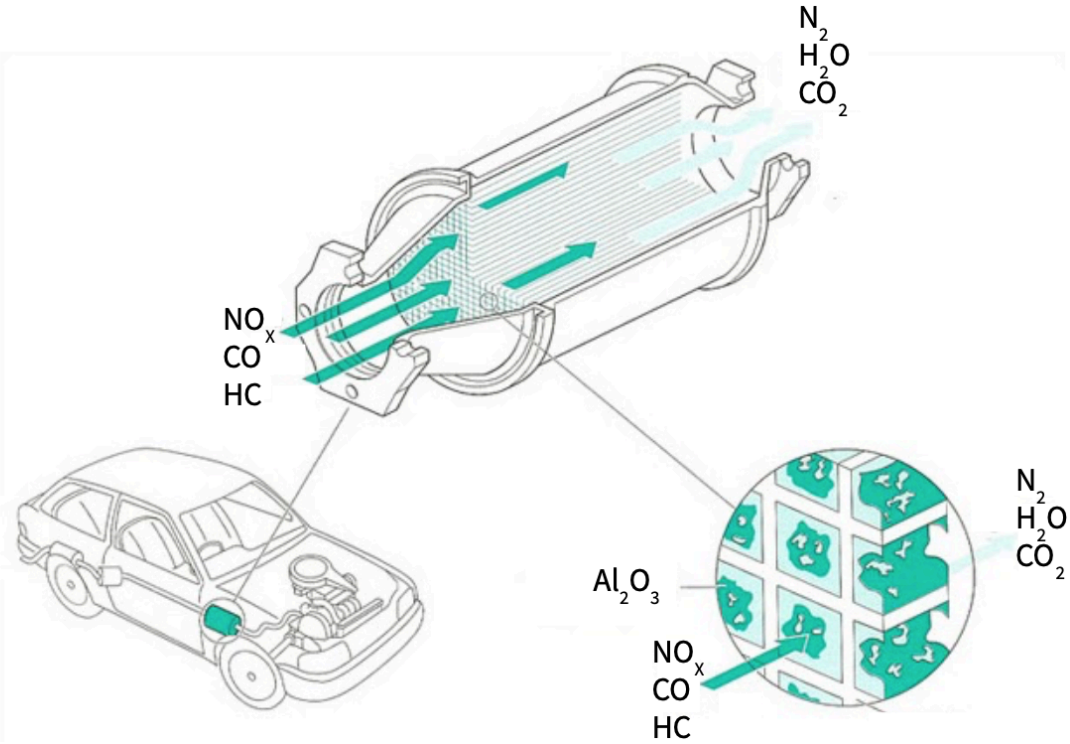

Figure 1-2: Gas flow through an automotive catalytic converter [24]
The three-way catalytic converter. An OpenLearn chunk used/reworked by permission of The Open University copyright © 2016. Courtesy of Dr S. Golunski, Johnson Matthey https://www.open.edu/openlearn/ocw/mod/oucontent/view.php?id=2492&extra=thumbnailfigure_idm45716837656816.

The process in which hydrocarbon combustion occurs within the catalytic converter is related to the generic combustion of volatile organic compounds (VOC). To determine efficiency of VOC oxidation there must be good catalytic activity, selectivity and stability [18]. VOC catalysts are promising ways to oxidize hydrocarbons due to the relatively low temperature at which the reaction will proceed. The light-off temperature needed for catalytic conversion is inversely proportional to the reactivity of the hydrocarbon [25]. The light-off temperature is defined as the temperature in which 50%

conversion of the pollutant is efficiently achieved [4]. A generic gas-phase hydrocarbon oxidation reaction is: $HC + O_2 \rightarrow CO_2 + H_2O$, in which the carbon dioxide and water vapor leave the catalytic converter as tailpipe emissions [25].

Carbon monoxide exhaust emissions are mitigated by hydration reactions. Carbon monoxide hydration is dependent on catalytic surface area and gas space velocity and is overall dependent on mass transfer. A carbon monoxide hydration reaction, $CO + H_2O \rightarrow CO_2 + H_2$, will occur under the proper conditions but produces a significant amount of vibrational energy. If the catalytic converter is not properly secured in the automobile, mechanical disturbances can possibly affect the overall activity, selectivity and function when converting carbon monoxide [25].

Nitric oxide (NO) reduction reactions can be very sensitive to debris and dust in the system and in some cases can decrease the conversion by 20%, which is another reason to make sure the catalytic converter is clean and properly selective [25]. When a catalytic converter is functioning normally the nitric oxide is reduced and the reaction is: $2NO + O_2 \rightarrow 2NO_2$.

It is important to ensure the catalytic converter is functioning properly. This is tested in most yearly automobile inspections. Catalytic converters need periodic maintenance and chemical cleaning, such as an alkaline wash. If the activity of catalytic converters is properly monitored and if they are cleaned when needed they can last upwards of 10 years [25].

Recent studies have shown the negative impacts PGEs have on the environment. Even when incorporated into the catalyst, PGE particles are still emitted into the environment (soil, vegetation) and atmosphere. In 2011, a study was conducted to see

how PGE were applied and results show that 36% of Pt used, 64% of Pd used and 78% of Rh used were used to create catalytic converters [26]. The release of high PGE concentrations in the environment has been linked to some biotoxicity. When screening adults in high-traffic and low-traffic areas, it was seen that adults in high-traffic areas had trace Pt and Rh in their urine whereas individuals in low-traffic areas did not. Pd and Rh concentrations were also found in the urine of children from the high-traffic areas. A correlation has been found that toxic effects of Pt, Pd, and Rh have been linked to increased risk of mutation, which can lead to tumorigenesis [26].

Application of Catalytic Aerogels to Catalytic Converters

Depletion of natural resources such as precious metals and increasing health risks associated with exposure to highly concentrated PGEs are a main reason that a substitute for catalytic converters containing PGEs are necessary for our society. Recent publications have shown that silica aerogels present minimal biotoxicity with exposure, not ingestion. However, in regard to environmental application our society is changing towards a circular economy, which means we need to manage our resources more efficiently. Aerogel technology is a very highly researched field and many advancements and innovations have been made in regard to the environment and life sciences. The continued research and application of aerogels will help bring our society towards smarter and cleaner solutions [27].

The ability to replace PGE with highly active, selective and sensitive TMOs in the catalytic converter of an automobile would begin to make progress towards cleaner products that are less destructive to the environment and have less of an effect on living organisms. There are over 1 billion automobiles in use around the world, the mitigation

of toxic emissions by application of the catalytic converter significantly changed and benefited our biome, but further modification needs to be made to the catalytic converters to continue to decrease the effects automobiles have on the global environment.

Chromia-based Aerogels

The successful fabrication and application of multiple different types of TMO aerogel catalysts has led to continued research to synthesize and test a variety of other transition metals to determine if they also have catalytic abilities. Chromia-based aerogel catalysts are now being explored due to bulk chromia having the highest specific activity in catalytic applications when compared to all other TMOs [18]. This could be due to the four different cationic oxidation states chromia exhibits in its favorable redox chemistry. The most common oxidation states of chromium are 3+, 6+, 2+, 4+, and zero [28]. For example, Cr^{3+} is found in octahedral crystal fields while Cr^{4+} is commonly seen in amorphous chromia (CrO_3) [10]. Chromia also presents favorable acid-base chemistry. These favorable characteristics of chromia result in successful oxygen chemisorption and high conversion rates when catalytic abilities were tested [18].

A research group in Israel has performed significant research on bulk chromia aerogel catalysts [9, 12, 18]. Bulk chromia catalysts form a hexagonal α- Cr_2O_3 crystalline structure, which is known as chromia eskolaite [10, 18]. Chromia can also form an octahedral lattice as $[Cr(OH)_3O_3]$ in which two-dimensional, distorted nanocrystal fragments of α-CrOOH, with no bonding on the Z-axis have been found [18]. A defining characteristic of these structures is bimodal pore size distributions, in which the crystals do not block or inhibit reactions within the mesoporous structure. The bulk chromia catalysts have a high surface area of about 600 m^2/g, which enhances the

activity, selectivity and stability of the aerogel [9]. It has further been found that addition of other trace metals such as Pt, Ce, Au, Mn increases the activity of chromia catalysts [12]. Little research has been conducted to determine the occupied and unoccupied electronic states of chromia aerogels [10].

Bulk chromia aerogels present favorable catalytic abilities and have been seen to out-perform other TMO bulk aerogels [9]. However, little to no research has been conducted incorporating chromia into aerogels with an alumina or silica backbone. Furthermore, only supercritical drying techniques at 90 °C and 85 mbar for four hours with overnight drying at 110 °C have been used to produce chromia aerogels [9,12,18]. The object of this thesis project is to investigate whether catalytic chromia-alumina and chromia-silica catalysts prepared via the RSCE method have properties that would render them suitable as substitutes for PGE in catalytic converters.

Characterization and Testing of Chromia-based Aerogels

In order to test the catalytic abilities of aerogels as a suitable substitute for PGE in a catalytic converter, our group has designed and constructed the Union Catalytic Testbed (UCAT). The testbed mimics the conditions of a catalytic converter found in an automobile using a unique blend of gases. A schematic can be seen in Figure 1-3 [29].

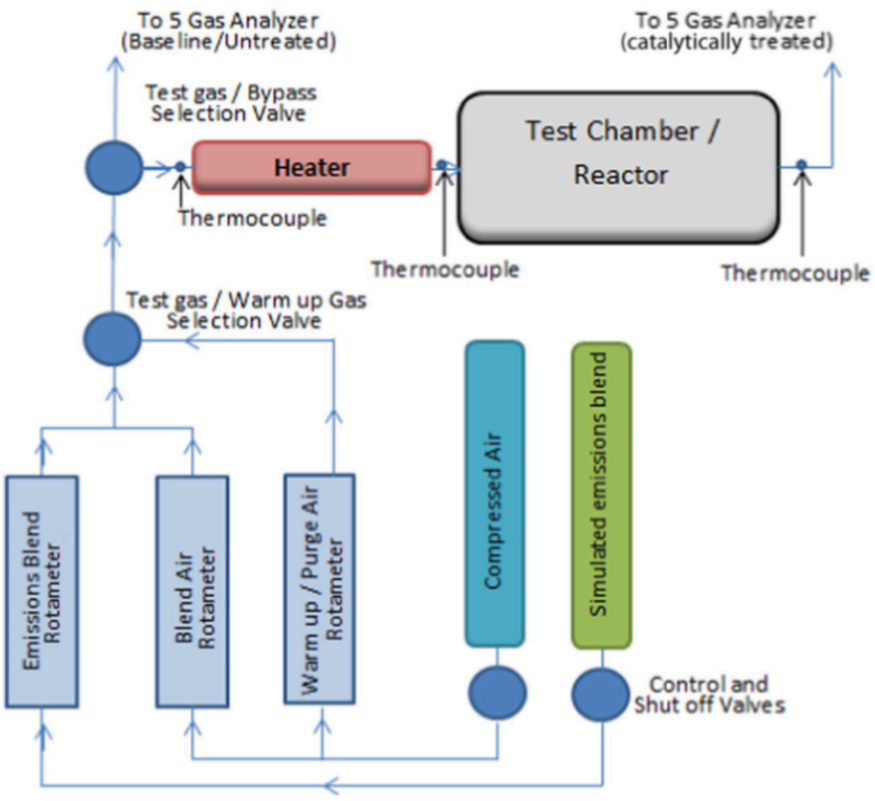

Figure 1-3: Schematic representation of the UCAT to mimic conditions and reactions seen in an automotive catalytic converter [15]. Juhl, S. J.; Dunn, N. J.; Carroll, M. K.; Anderson, A. M.; Bruno, B. A.; Madero, J. E.; Bono, M. S. Epoxide-Assisted Alumina Aerogels by Rapid Supercritical Extraction. *Journal of Non-Crystalline Solids* **2015**, *426*, 141–149.

In order to characterize the surface area, pore size and pore distribution of chromia aerogels the Micromeritics ASAP 2020 Surface Area and Porosity Analyzer is used. X-ray Powder Diffraction (XRD) can be used to determine the crystalline structure and dispersion of chromia within the aerogel. Scanning Electron Microscopy (SEM) can also be used to provide detailed information about the surface of nanostructures and further the chemical composition and elemental mapping of the nanoparticles using Energy-dispersive X-Ray Spectroscopy (EDS). These techniques will give us insight into the nanostructure of chromia based aerogels and allow for a better understanding of their catalytic abilities and hopeful application.

In this thesis I outline an effective chromia-based aerogel fabrication technique using the Union College RSCE technique. The resulting chromia-based aerogels are physically and chemically characterized using a number of techniques and catalytic ability is determined using the Union College Catalytic Testbed. These are very promising nanomaterials due to their high surface area, high pore volume, low density and high activity. They present as a viable substitute for conventional three-way catalysts (TWC) due to the present issues in regard to the cost and environmental impact of current automotive TWC.

Introduction References

[1] Pierre, A. C.; Rigacci, A. "SiO_2 Aerogels." In *Aerogels Handbook,* Aegerter, M. A., Leventis, N. and Koebel, M. (Eds.); Springer: New York, NY, 2011.

[2] Reprinted by permission from Springer Nature Customer Service Centre GmbH: Springer. Aerogels Handbook, "Sodium Silicate Based Aerogels via Ambient Pressure Drying." Venkateswara Rao, A.; Pajonk, G. M.; Bangi, Uzma K. H.; Parvathy Rao, A., Koebel, M. M. © Springer Science + Business Media, LLC 2011 DOI 10.1007/978-1-4419-7589-8.

[3] Pierre, A. C. "History of Aerogels" In *Aerogels Handbook,* Aegerter, M. A., Leventis, N. and Koebel, M. (Eds.); Springer: New York, NY, 2011.

[4] Posada, L. F.; Carroll, M. K.; Anderson, A. M.; Bruno, B. A. Inclusion of Ceria in Alumina- and Silica-Based Aerogels for Catalytic Applications. *The Journal of Supercritical Fluids* **2019**, *152*, 104536.

[5] Durães, L.; Oliveira, O.; Benedini, L.; Costa, B. F.; Beja, A. M.; Portugal, A. Sol–Gel Synthesis of Iron(III) Oxyhydroxide Nanostructured Monoliths Using $Fe(NO_3)_3 \cdot 9H_2O/CH_3CH_2OH/NH_4OH$ Ternary System. *Journal of Physics and Chemistry of Solids* **2011**, *72*(6), 678–684.

[6] Baumann, T. F.; Gash, A. E.; Chinn, S. C.; Sawvel, A. M.; Maxwell, R. S.; Satcher, J. H. Synthesis of High-Surface-Area Alumina Aerogels without the Use of Alkoxide Precursors. *Chemistry of Materials* **2005**, *17*(2), 395–401.

[7] Boumaza, A., Favaro, L Lédion, J, Sattonnay, J. Brubach, P, Berthet, A, Huntz, P, & Tétot, R. "Transition Alumina Phases Induced by Heat Treatment of Boehmite: An X-ray Diffraction and Infrared Spectroscopy Study." Journal of Solid State Chemistry 182 (2009): 1171-1176.

[8] Bouck, R. M.; Anderson, A. M.; Prasad, C.; Hagerman, M. E.; Carroll, M. K. Cobalt-Alumina Sol Gels: Effects of Heat Treatment on Structure and Catalytic Ability. *Journal of Non-Crystalline Solids* **2016**, *453*, 94–102.

[9] Landau, M. V.; Shter, G. E.; Titelman, L.; Gelman, V.; Rotter, H.; Grader, G. S.; Herskowitz, M. Alumina Foam Coated with Nanostructured Chromia Aerogel: Efficient Catalytic Material for Complete Combustion of Chlorinated VOC. *Industrial & Engineering Chemistry Research* **2006**, *45*(22), 7462–7469.

[10] Kucheyev, S. O.; Sadigh, B.; Baumann, T. F.; Wang, Y. M.; Felter, T. E.; Buuren, T. V.; Gash, A. E.; Satcher, J. H.; Hamza, A. V. Electronic Structure of Chromia Aerogels fromSoft x-Ray Absorption Spectroscopy. *Journal of Applied Physics* **2007**, *101*(12).

[11] Pareek, A.; Mohan, S. V. Graphene and Its Applications in Microbial Electrochemical Technology. *Microbial Electrochemical Technology* **2019**, 75–97.

[12] Rotter, H.; Landau, M. V.; Herskowitz, M. Combustion of Chlorinated VOC on Nanostructured Chromia Aerogel as Catalyst and Catalyst Support. *Environmental Science & Technology* **2005**, *39*(17), 6845–6850.

[13] Baumann, T. F.; Gash, A. E.; Satcher Jr, J. H. "A Robust Approach to Inorganic Aerogels: The Use of Epoxides in Sol–Gel Synthesis." In *Aerogels Handbook,* Aegerter, M. A., Leventis, N. and Koebel, M. (Eds.); Springer: New York, NY, 2011.

[14] Armor, J. N.; Carlson, E. J. Variables in the Synthesis of Unusually High Pore VolumeAluminas. *Journal of Materials Science* **1987**, *22*(7), 2549–2556.
[15] Juhl, S. J.; Dunn, N. J.; Carroll, M. K.; Anderson, A. M.; Bruno, B. A.; Madero, J. E.; Bono, M. S. Epoxide-Assisted Alumina Aerogels by Rapid Supercritical Extraction. *Journal of Non-Crystalline Solids* **2015**, *426*, 141–149.
[16] Karami, D. A Review of Aerogel Applications in Adsorption and Catalysis. *Journal of Petroleum Science and Technology* **2018**, *8*(4), 3–15.
[17] Wallace, J. World's Most Expensive Precious Metal Surges Amid Emissions Clampdown. *The Wall Street Journal* **2020**. (https://www.wsj.com/articles/worlds-most-expensive-precious-metal-surges-amid-emissions-clampdown-11579780770)
[18] Rotter, H.; Landau, M.; Carrera, M.; Goldfarb, D.; Herskowitz, M. High Surface Area Chromia Aerogel Efficient Catalyst and Catalyst Support for Ethylacetate Combustion. *Applied Catalysis B: Environmental* **2003**, *47*(2), 111–126.
[19] Tobin, Z. M.; Posada, L. F.; Bechu, A. M.; Carroll, M. K.; Bouck, R. M.; Anderson, A. M.; Bruno, B. A. Preparation and Characterization of Copper-Containing Alumina and Silica Aerogels for Catalytic Applications. *Journal of Sol-Gel Science and Technology* **2017**, *84*(3), 432–445.
[20] Smith, L. C.; Anderson, A. M.; Carroll, M. K. Preparation of Vanadia-Containing Aerogels by Rapid Supercritical Extraction for Applications in Catalysis. *Journal of Sol-Gel Science and Technology* **2015**, *77*(1), 160–171.
[21] Bruno, B. A.; Madero, J. E.; Juhl, S. J.; Rodriguez, J.; Dunn, N. J. H.; Carroll, M. K.; Anderson, A. M. "Alumina-Based Aerogels as Three-Way Catalysts." Conference proceedings of the Ninth International Congress on Catalysis and Automotive Pollution Control (CAPoC9), August 2012.
[22] Heck, R. M.; Farrauto, R. K. *"Catalytic Air Pollution Control: Commercial Technology", 3rd Edition*. *Platinum Metals Review* **2010**, *54*(3), 180–183.
[23] Amatayakul, W., Ramnäs, O. Life cycle assessment of a catalytic converter for passenger cars. *J. Clean. Prod*. **2001** 9(5). 395– 403
[24] The three-way catalytic converter. An OpenLearn chunk used/reworked by permission of The Open University copyright © 2016. Courtesy of Dr S. Golunski, Johnson Matthey https://www.open.edu/openlearn/ocw/mod/oucontent/view.php?id=2492&extra=thumbnailfigure_idm45716837656816.
[25] Farrauto, R.J., Bartholomew, C.H. Fundamentals of Industrial Catalytic Processes, Blackie Academic, London, 1997, pp. 635–650.
[26] Wang, Y.; Li, X. Health Risk of Platinum Group Elements from Automobile Catalysts. *Procedia Engineering* **2012**, *45*, 1004–1009.
[27] García-González, C. A.; Budtova, T.; Durães, L.; Erkey, C.; Gaudio, P. D.; Gurikov, P.; Koebel, M.; Liebner, F.; Neagu, M.; Smirnova, I. An Opinion Paper on Aerogels for Biomedical and Environmental Applications. *Molecules* **2019**, *24*(9), 1815.
[28] Chromium - Element information, properties and uses: Periodic Table. *Royal Society of Chemistry* https://www.rsc.org/periodic-table/element/24/chromium (accessed Feb 5, 2020).
[29] Gurian, Tyler. Assembly and Testing of the Second Generation Union Catalytic Testbed, Union College, 2016.

2. EXPERIMENTAL

Wet Gel Fabrication via Epoxide-assisted Method

Chromia-based catalytic aerogels with an alumina backbone were fabricated using both an impregnation method and a co-precursor method. The impregnation synthesis method was adapted from Juhl et al. [1] and Posada et al. [2]. A 2.96-g aliquot of aluminum chloride hexahydrate ($AlCl_3 \cdot 6H_2O$) (Fisher, 99% purity) was added to 20 mL of reagent-grade ethanol (Fisher Scientific, 99%) and stirred with a stir bar; the salt fully dissolved after 20-45 minutes. While stirring 4.82 mL of propylene oxide (Sigma Aldrich, >99%; safety note: toxic and a probable human carcinogen) was added to the solution and stirred until gelation occurred (within seven minutes of propylene oxide addition.

The co-precursor synthesis technique was adapted from Baumann et al. 2005 [3] and Posada et al. 2019 [2]. A 2.96-g aliquot of $AlCl_3 \cdot 6H_2O$ was dissolved in 20 mL of reagent-grade ethanol and stirred with a stir bar until the salt dissolved completely (20-45 minutes). In a separate beaker, 0.98 grams of $Cr(NO_3)_3 \cdot 9H_2O$ (Mallinckrodt, analytical reagent) was added to 20 mL of reagent-grade ethanol, stirred with a stir bar and dissolved in 7-15 minutes. Once both salts were dissolved, the solutions were mixed together and allowed to stir for 2 minutes. The resulting co-precursor salt solution is a 5:1 mole ratio of aluminum salt to chromium salt. While stirring, 8.50 mL of propylene oxide was added to the mixture and allowed to stir for 15 min. Next, the solution was removed from the stir plate. Gelation occurred within 20 minutes of the addition of propylene oxide.

Investigation of Alternate Gelation Method

Durães et al. [4] proposed an alternate proton scavenger to propylene oxide that is less toxic, carcinogenic and volatile: ammonium hydroxide. This approach was adapted and used to determine if 10-M ammonium hydroxide would induce gelation in a chromium nitrate nonahydrate solution without alumina or silica present in the solution. 1.97 g of $Cr(NO_3)_3 \cdot 9H_2O$ was stirred until dissolved in 10 mL of reagent grade ethanol (30 minutes). The solution was heated to 60 °C. A 10-M solution of weak base was prepared via dilution of 15-M ammonium hydroxide (Fisher Scientific, 35% Ammonium Hydroxide) with DI water and then added dropwise to the mixture. However, before gelation could occur a white precipitate formed in the solution and addition of ammonia was stopped. No data from the literature has shown that ammonia can induce gelation of a chromia-ethanol solution.

Solvent Exchanges

Once gelation has occurred, the sol-gel was allowed to sit in the beaker covered with Parafilm ® for 48 h under ambient conditions. Then, three solvent exchanges were performed, as described below. If using the impregnation method, the first solvent exchange was performed with a solution of 2.00 grams of $Cr(NO_3)_3 \cdot 9H_2O$ dissolved in 20 mL of absolute ethanol (Pharmco-AAPER) instead of cerium salt as stated by Posada et al. [2]. All other solvent exchanges used 20 mL of absolute ethanol. All three solvent exchanges performed on sol-gels formed via co-precursor synthesis techniques used absolute ethanol.

48 h after gelation, the excess solvent in the beaker was decanted and the sol-gel was broken into small pieces. Then, 20 mL of absolute ethanol (or 10% w/v of chromium salt in absolute ethanol) was added to the gel, and the beaker containing the gel was covered in Parafilm ® and allowed to sit at ambient conditions. 48 h later, the excess solvent in the beaker was decanted and 20 mL of absolute ethanol was added. This was repeated for the third time 48 h later to complete a sequence of three solvent exchanges.

Rapid Supercritical Extraction (RSCE)

Once the solvent exchanges were complete, the sol-gel sample was placed in the wells of a stainless-steel mold. Two stainless-steel molds were used throughout the course of this project. Mold 1 is a 5” x 5” slab of stainless steel with four wells, each with a diameter of 1.5” and depth of 0.63”. Mold 2 is a 5” x 5” slab of Easy-to-Machine 416 Stainless Steel (McMaster Carr) with four wells, each with a diameter of 1.60” and depth of 0.63”. Mold 1 and Mold 2 are depicted side by side in Figure 2-1 and the design of Mold 2 is presented in Figure 2-2.

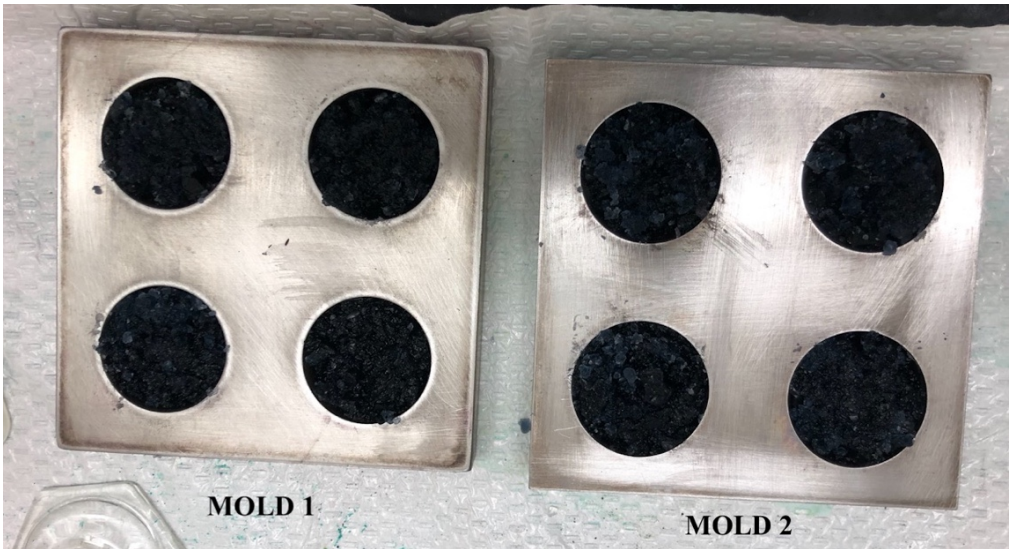

Figure 2-1: Mold 1 (L) is characterized by a smaller well volume compared to Mold 2 (R). The wells of the two molds contain chromia-alumina wet gels.

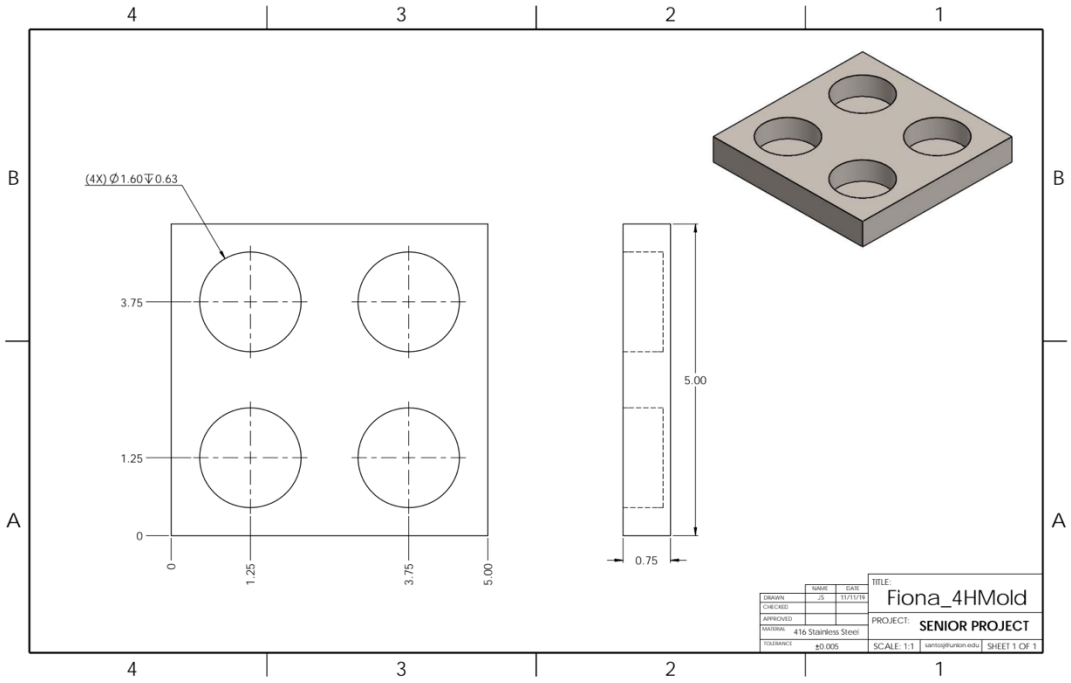

Figure 2-2: Stainless-steel Mold 2 design used for treatment of sol-gel samples in the hydraulic hot press, courtesy of Joana Santos (Mechanical Engineering Department, Union College).

Each well was filled with chromia-alumina wet gel (without being tightly packed down) and topped off with absolute ethanol. A compressed NOVATEC 825F Engineered Graphite graphite gasket (Phelps Gaskets) was placed under the mold before being put in the hydraulic hot press and then sealed with 6 x 6" stainless steel foil (Brown Metals Company 0.0005 x 6.000") and 6 x 6" graphite gasket, with a thickness of 0.072". To achieve rapid supercritical extraction of ethanol from the wells, the 50-ton hydraulic hot press (Accudyne Inc.) induced a restraining force and temperature ramp on the sealed, constant-volume mold. This caused the pressure to increase and the solvent, ethanol, became a supercritical fluid. The critical temperature of ethanol is about 470 °F (243.3 °C) and the critical pressure is 6.390 MPa [5]. The mold was held well above the critical temperature and pressure of ethanol as described in Step 2 of the hydraulic hot press

parameters shown in Table 2-1. The restraining force and temperature was decreased and the supercritical solvent escaped the mold and left behind aerogels [6]. All parameters for use of the hydraulic hot press are outlined in Table 2-1.

Table 2-1. Hydraulic hot-press parameters for chromia-alumina aerogel fabrication.

Step #	Temperature		Rate of Temperature		Force		Rate of Force		Time (min)
	(°F)	(°C)	°F/min	°C/min	Kips	kN	Kips/min	kN/min	
1	90	32	200	111	45	200	45	200	0
2	480	250	6	3.3	45	200	45	200	30
3	480	250	200	111	1	4.5	1	4.5	15
4	90	38	6	3.3	1	4.5	1	4.5	0
5	0	0	0	0	0	0	0	0	0

Aerogel Calcination

High temperature heat-treatment is performed on aerogel samples to ensure the samples' structure and oxidation state do not change during subsequent catalytic testing. The samples were placed in ceramic crucibles with lids and heated for 24 h at 800 °C in a Thermolyne furnace. The furnace was allowed to heat up to 800 °C and samples were added when at temperature.

The mass and volume of fabricated chromia-alumina aerogels were measured before and after calcination to determine the change in density. Masses were measured with an Explorer Pro Analytical Balance and volumes were estimated using a graduated cylinder. This method does not account for the volume of void space between aerogel granules and, therefore, overestimates volume and underrepresents density.

X-ray Powder Diffraction

Aerogel samples as prepared and post calcination were ground into a fine powder with a mortar and pestle to characterize via X-ray powder diffraction using a Rigaku Smartlab SE XRD with a Cu Kα source. The aerogel powder was placed in a glass plate with a 0.5-mm well and placed in the XRD instrument to analyze the diffraction patterns under General (BB) mode using the parameters in Table 2-2. The peak-matching software is 4.3.128.0 Smart Lab Studio II.

XRD analysis was also conducted while heating samples with a furnace inside the instrument to understand the changes in the crystalline structure as temperature increases (every 100 °C). As-prepared chromia aerogel samples were ground with a mortar and pestle and placed on a 4-mm ceramic disk. The ceramic disk was placed in a Parr 1200 sample oven, secured with an aluminum clip and placed in the XRD. The temperature ramp started at room temperature (26 °C) and was increased every ten minutes, with a five-minute hold once at temperature. Temperature ramp studies were performed until the sample within the Parr 1200 oven reached 800 °C.

Table 2-2. XRD experimental parameters.

Start (°)	End (°)	Step (°)	Speed (°/min)	Incident slit (°)	Receiving slit (mm)
5.0000	80.0000	0.0300	15.0	1.0	20.000

Surface Area Analysis

The Micromeritics ASAP 2020 Surface Area and Porosity Analyzer was used to characterize the total surface area and pore volume of aerogels as prepared and post calcination. Aerogel samples were prepared by lightly crushing and then degassing at 90

°C for 2 hours and 200 °C for 6 hours (Table 2-3). All analysis conditions are as presented in Tables 2-3 through 2-9.

Table 2-3: Degas conditions

Evacuation Phase:		**Heating Phase:**	
Temperature Ramp Rate	10.0 °C/min	Ramp rate	10.0 °C/min
Target Temperature	90 °C	Hold temp	200 °C
Evacuation Rate	5.0 mmHg/s	Hold time	360 min
Unrestricted evac. from	5.0 mmHg		
Vacuum setpoint	25 µmHg	**Evacuation and Heating Phase:**	
Evacuation Time	120 min	Hold Pressure	100 mmHg

Table 2-4: Analysis Preparation

Unrestricted evac. from	5.0 mmHg
Vacuum setpoint	10 µmHg
Evacuation time	0.10 h
Leak test duration	120 s

Note: Boxes for Fast evacuation, Leak test, Use TransSeal should NOT be checked off.

Table 2-5: Free Space

⊙ Measure		
✓	Lower dewar for evacuation	
	Evacuation time	0.10 h
NO CHECK	Outgas test	
	Outgas test duration	180 s
○ Enter		
	Warm free space	16.0000 cm3
	Cold free space	45.0000 cm3
○ Calculate		

Table 2-6: p° and temperature options

⊙	1. Measure p° at intervals during analysis. Calculate the Analysis Bath Temperature from these values.	
○	2. Measure p° at intervals during analysis. Enter the Analysis Bath Temperature below.	
○	3. Enter p° below. Calculate the Analysis Bath Temperature at the time of analysis.	
○	4. Enter p° below. Enter the Analysis Bath Temperature below.	
○	5. Measure Psat of a gas. Calculate p° of the adsorptive from the measured Psat. Calculate the Analysis Bath Temperature using the Adsorptive Properties temperature data	
○	6. Calculate p° (using Adsorptive Properties temperature data) at the time of the analysis from the Analysis Bath Temperature entered below	
	Ambient Temperature	22.00 °C
	Measurement interval	120 min

Table 2-7: Dosing options

First pressure fixed dose	0.0100 cm^3/g STP
Maximum volume increment	25.00000 cm^3/g STP
Absolute pressure tolerance	5.000 mmHg
Relative pressure tolerance	5.0 %
Low Pressure incremental dose mode	
Dose amount	0.0100 cm^3/g STP
Equilibration Delay	
Minimum	0.00 h
Maximum	999.00 h

Table 2-8: Equilibration

Relative Pressure (p/p°)	Equilibration Intervals (s)		
0.900000000	20	Time	600 s
0.995000000	35		

Table 2-9: Sample backfill options

✓	Backfill sample at start of analysis
✓	Backfill sample at end of analysis
Backfill gas:	N_2

Scanning Electron Microscopy & Energy-Dispersive X-ray Spectroscopy

A Zeiss EVO MA15 was used to analyze as-prepared and post-calcined aerogels via Scanning Electron Microscopy (SEM) and Energy-dispersive X-ray Spectroscopy (EDS) imaging. Sample were prepared by mounting packed-down powdered aerogel onto carbon tape. Standard parameters of 12 kV EHT and 500 spot size were used to collect EDS images whereas a voltage of 15 kV and a spot size of 300 were used to collect SEM images.

Catalytic Testing: UCAT

Catalytic testing was conducted using the Union Catalytic Aerogel Testbed (UCAT) on post-calcined chromia aerogel samples. Samples were tested under two conditions: high air (O_2%, 1.15%) or low air (O_2%, 0.12%). Gas pollutant mixtures in high air or low air were flowed through the sample, which was held in a steel sample holder. Gas was allowed to flow through the sample for 3 min before taking a reading. Gas pollutant concentrations for low-air and high-air gas mixtures are expressed in Table 2-10 and UCAT test parameters are presented in Table 2-11.

Table 2-10: Simulated Exhaust Gas Pollutant Concentrations

CLEERS DRY GAS FORMULATION		
[gas]	Low air (λ= 0.97)	High air (λ= 1.02)
O_2 (ppm)	1200	11500
Propene (ppm)	1180	1130
NO (ppm)	1180	1130
CO (ppm)	5920	5630
CO_2 (ppm)	154000	146000
H_2 (ppm)	2010	1910

Note: Lambda (λ) is a measure used in the automotive industry of how close a fuel air mixture is to stoichiometric. The composition of the exhaust and the pollutants formed strongly depends on lambda. $\lambda > 1$ means the combustion is fuel lean and $\lambda < 1$ means the combustion is fuel rich.

Table 2-11: UCAT testing parameters

Input	Values
Reactor Volume	20 mL wall, 17 mL door
Space Velocity	20
Standard Temperature (K)	298
Temperature Range (°C)	200-600
ΔT (°C)	50

Experimental References

[1] Juhl, S. J.; Dunn, N. J.; Carroll, M. K.; Anderson, A. M.; Bruno, B. A.; Madero, J. E.; Bono, M. S. Epoxide-Assisted Alumina Aerogels by Rapid Supercritical Extraction. *Journal of Non-Crystalline Solids* **2015**, *426*, 141–149.

[2] Posada, L. F.; Carroll, M. K.; Anderson, A. M.; Bruno, B. A. Inclusion of Ceria in Alumina- and Silica-Based Aerogels for Catalytic Applications. *The Journal of Supercritical Fluids* **2019**, *152*, 104536.

[3] Baumann, T. F.; Gash, A. E.; Chinn, S. C.; Sawvel, A. M.; Maxwell, R. S.; Satcher, J. H. Synthesis of High-Surface-Area Alumina Aerogels without the Use of Alkoxide Precursors. *Chemistry of Materials* **2005**, *17*(2), 395–401.

[4] Durães, L.; Oliveira, O.; Benedini, L.; Costa, B. F.; Beja, A. M.; Portugal, A. Sol–Gel Synthesis of Iron(III) Oxyhydroxide Nanostructured Monoliths Using $Fe(NO_3)_3 \cdot 9H_2O/CH_3CH_2OH/NH_4OH$ Ternary System. *Journal of Physics and Chemistry of Solids* **2011**, *72*(6), 678–684.

[5] Price, P. Physical Property Data for the Design Engineer. *The Chemical Engineering Journal* **1989**, 42 (1), 70–71.

[6] Bono, M. S.; Anderson, A. M.; Carroll, M. K. Alumina Aerogels Prepared via Rapid Supercritical Extraction. *Journal of Sol-Gel Science and Technology* **2009**, 53(2), 216–226.

3. RESULTS

Wet Gel Fabrication

The impregnation technique, in which the first solvent exchange contained chromium nitrate nonahydrate ($Cr(NO_3)_3 \cdot 9H_2O$) dissolved in absolute ethanol, did not gel properly. The alumina-based gel formed and the first solvent exchange was performed; however, 24 hours later when the second of three solvent exchanges was to be performed, it was noted that the gel had disintegrated and was more of a viscous liquid. This technique was then discontinued and the co-precursor technique was used to fabricate chromia-based aerogels.

When the co-precursor method was employed for chromia-based aerogel production, the aluminum chloride hexahydrate ($AlCl_3 \cdot 6H_2O$) salt solution produced was usually colorless and clear (translucent) but in some batches this solution turned a pale-yellow color as seen in Figure 3-1. This alumina solution color change was noted in some batch productions and was not linked to any differences seen in aerogel production or characterization. This color discrepancy is likely due to the dissolution being performed in contaminated or dirty glassware.

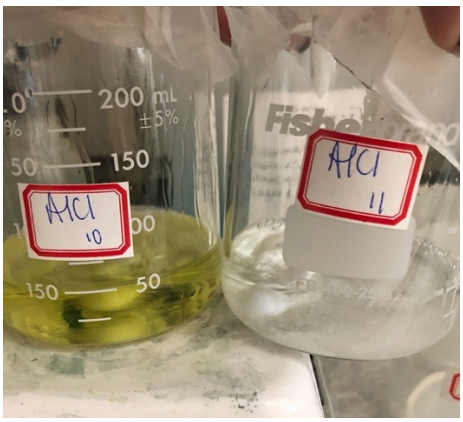

Figure 3-1: Aluminum chloride hexahydrate dissolved in reagent-grade ethanol occasionally produced translucent-yellow solutions (left) and, more commonly, translucent-colorless solutions (right).

Chromium (III) nitrate nonahydrate ($Cr(NO_3)_3 \cdot 9H_2O$) dissolved in reagent-grade ethanol in 7-15 minutes. The resulting solution was a dark, midnight-blue color. The aluminum salt solution and chromium (III) salt solution mixed together resulted in a non-translucent dark midnight-blue color but sometimes presented as a semi-translucent dark forest-green color when stirred for an extended period of time (or with addition of propylene oxide) as seen in Figure 3-2. The forest green chromium-aluminum solution had no correlation to arbitrary yellow color seen in some aluminum solutions.

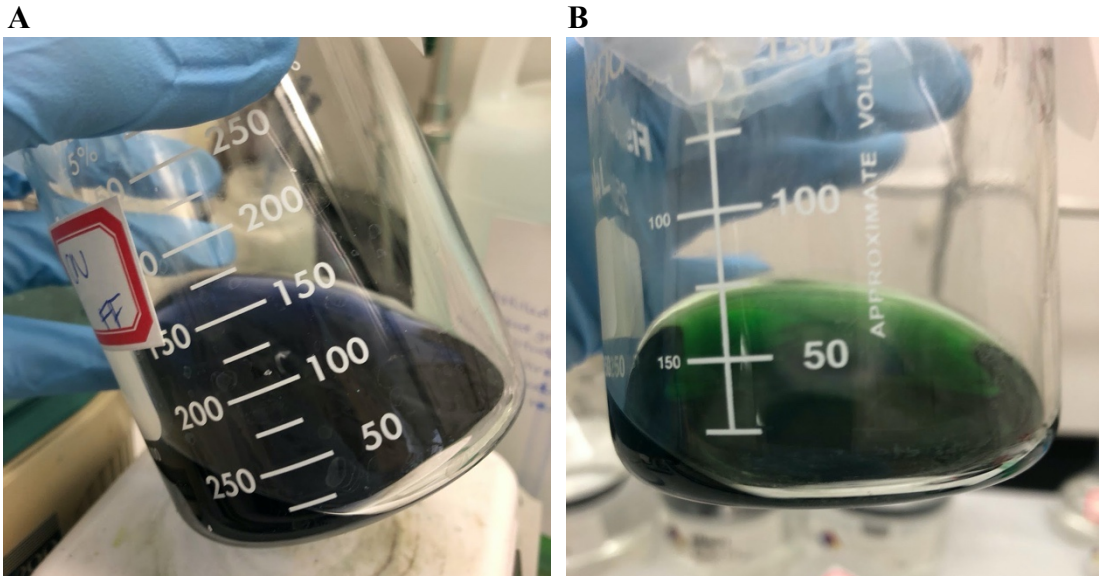

Figure 3-2: A mixture containing chromium nitrate nonahydrate dissolved in reagent-grade ethanol and aluminum chloride hexahydrate dissolved in reagent-grade ethanol produced solutions characterized by a dark, midnight-blue color (**A)** and, less frequently, a dark, forest-green color (**B**).

The addition of propylene oxide induced gelation within 20 minutes. Sometimes a color transition of dark midnight-blue color to dark forest-green color was noted with the addition of propylene oxide; however, the resulting gel was always a non-translucent dark midnight-blue color (Figure 3-3).

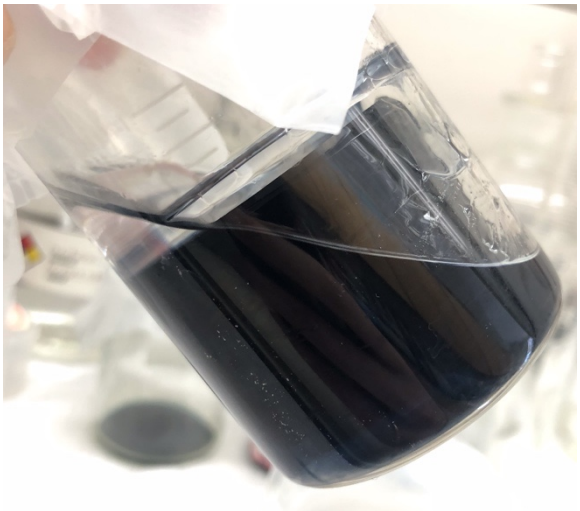

Figure 3-3: A chromia-alumina wet gel 48 hours after gelation occurred.

Solvent Exchanges

Three solvent exchanges were performed on the produced wet gels. The first of three occurred 48 hours after gelation; the solvent was decanted and the remaining wet gel was broken into small pieces using a spatula as shown in Figure 3-4.

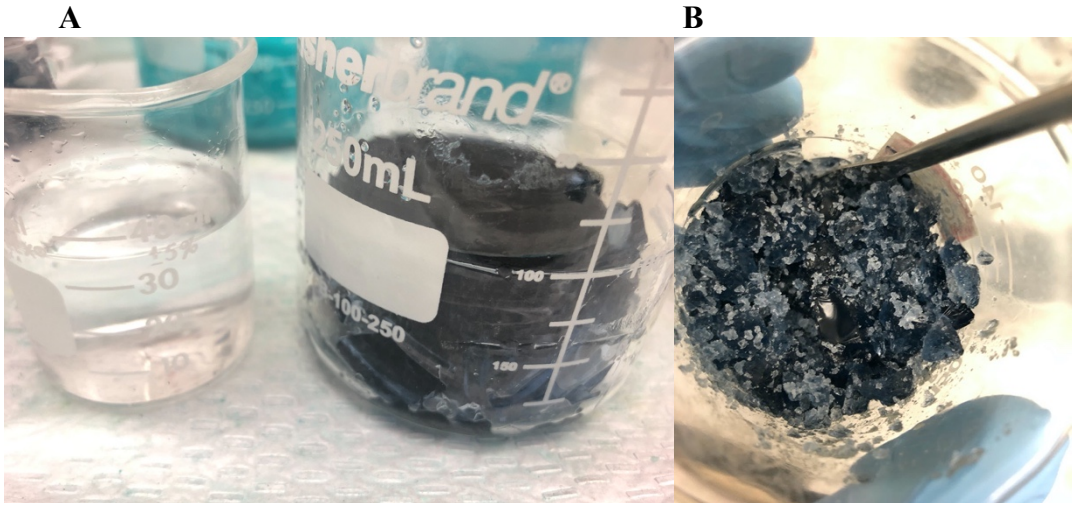

Figure 3-4: A depicts 40 mL of the decanted solvent (left beaker), which is completely colorless and shows no obvious loss of chromium ions, and the deeply-colored gel (right beaker). **B** depicts the fragmented wet-gel pieces.

The second solvent exchange occurred 48 hours after the first solvent exchange and solvent exchange three was performed 48 hours after the second solvent exchange. The decanted solvent from the second and third exchanges usually had a cloudy-blue color due to the presence of minuscule gel pieces lost through decanting, as shown in Figure 3-5.

Figure 3-5: The decanted solution (left) has a cloudy, translucent-blue color due to the loss of some small pieces of wet gel through the decanting process. The chromia-alumina wet gel is pictured on the right.

After the third solvent exchange the wet gel was allowed to sit in 40 mL of absolute ethanol for a minimum of 24 hours before the wet gel was processed using the rapid supercritical extraction process in the hydraulic hot press.

Rapid Supercritical Extraction

The solution was decanted off the wet gel, with minimal to no gel loss, and the wet gel was divided between four wells of the stainless-steel mold without packing down (Figure 3-6).

Figure 3-6: The chromia-alumina wet gel divided between the wells of the stainless-steel mold without packing down. Absolute ethanol was added to top off the wells (not pictured). This example uses "Mold 1" as depicted in Figure 2-1.

After processing through the hydraulic hot press, the volume of the as-prepared chromia-alumina aerogels was about 87% less than the estimated volume of wet gels before processing ($\%\ shrinkage = \frac{volume\ as\ prepared - volume\ post\ calcination}{volume\ as\ prepared}\ x\ 100$). The produced aerogels had a dark-green color with a lighter-green dusty coating as seen in Figure 3-7.

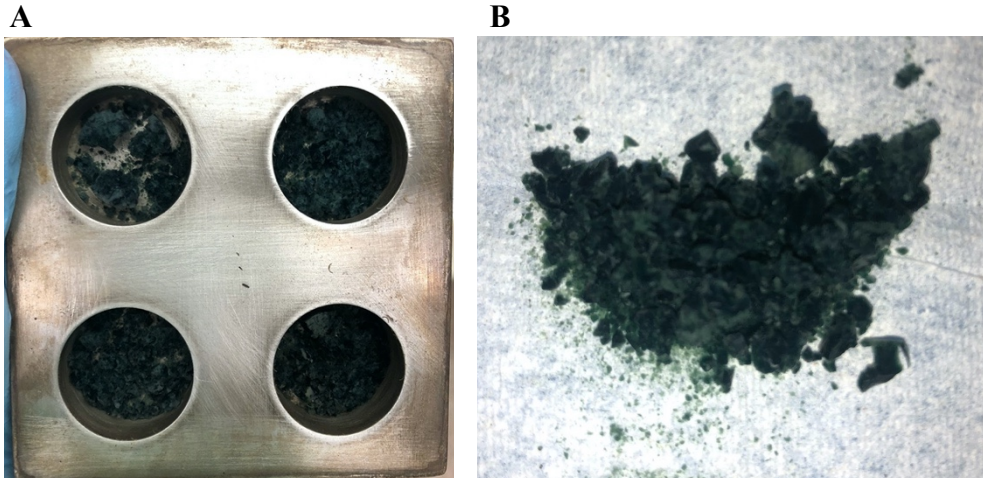

Figure 3-7: A observed shrinkage seen in processed, as-prepared chromia-alumina aerogels (Mold 1). Aerogels were covered in a dusty green powder. **B** depicts dark green chromia-alumina aerogel pieces after removal from the stainless-steel mold.

However, when using “Mold 2” depicted in Figure 2-1 and Figure 2-2, the aerogels produced were characterized by a darker-green color with a brown dust coating the samples, as seen in Figure 3-8.

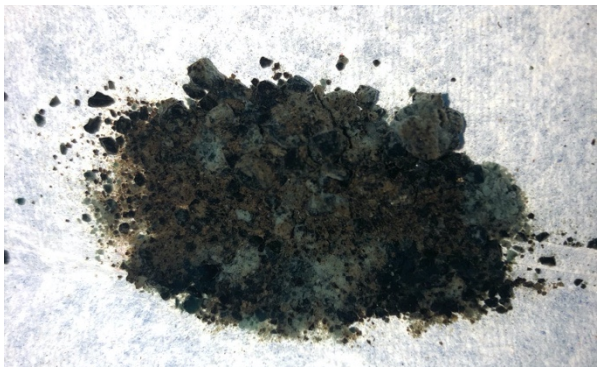

Figure 3-8: Chromia-alumina aerogels produced using a stainless-steel Mold 2 (Fig 2-2).

Aerogel Calcination

After RSCE processing, the mass and volume of aerogel samples were measured to determine the as-prepared density. The average density of aerogels as prepared was determined to be 0.21 ± 0.03 g/mL. After the aerogels were heated in the furnace at 800 °C for 24 hours the resulting calcined aerogels had a vibrant-green color (Figure 3-9) in contrast to their initial dark-green color (Figure 3-7B). The average density of aerogels post calcination was measured to be 0.30 ± 0.02 g/mL, indicating nearly a 50% increase in density post calcination. The shrinkage of chromia-alumina aerogels post calcination was measured to be about 55%.

Figure 3-9: Calcined chromia-alumina aerogels.

When “Mold 2” (depicted in Figure 2-1and Figure 2-2) was employed to produce the aerogels, a more drastic change in color change was seen following calcination, in comparison to aerogels made in “Mold 1.” Post-calcination samples are depicted in Figure 3-10, and show differences in color in comparison to the as-prepared samples shown in Figure 3-7B and 3-8.

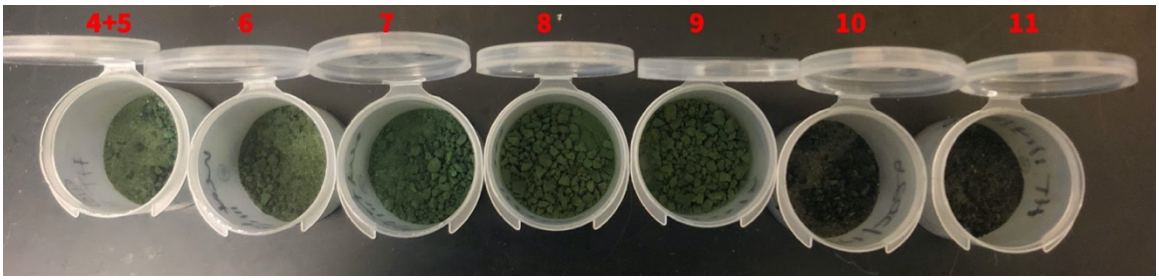

Figure 3-10: Samples labeled 4+5 to 9 represent aerogels produced in Mold 1. These have a vibrant-green color post-calcination. Samples labeled 10 and 11 were produced in Mold 2; the resulting aerogels post-calcination were a darker, cameo-green color. Images of Mold 1 and Mold 2 are depicted in Figure 2-1.

X-Ray Powder Diffraction

XRD analysis at room temperature was performed on aerogel samples pre- and post-calcination. Peaks observed for each sample were matched as shown in Figures 3-11 and 3-12. XRD analysis was also performed with a furnace within the instrument to create a temperature ramp while analyzing the as-prepared samples to determine changes in composition as the temperature was increased from room temperature (26 °C) to 800 °C. Figure 3-13 presents diffraction patterns observed at each stage of the temperature ramp.

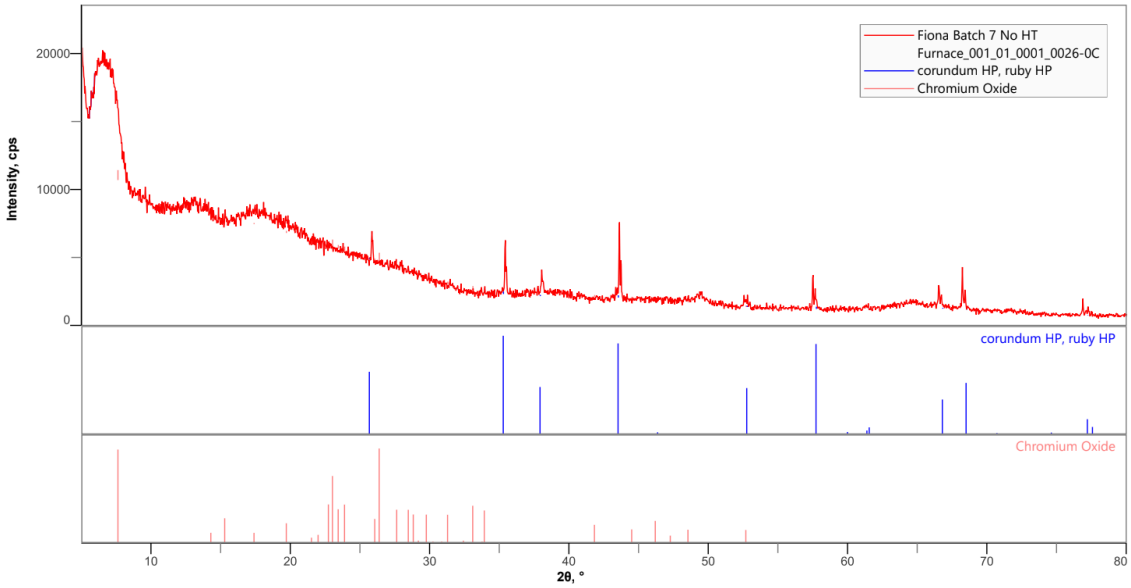

Figure 3-11: XRD pattern of chromia-alumina as-prepared aerogel sample. The matching software identified peaks due to corundum (blue), which is a mineral name for Al_2O_3, as well as peaks due to chromium oxide, Cr_3O_8 (pink).

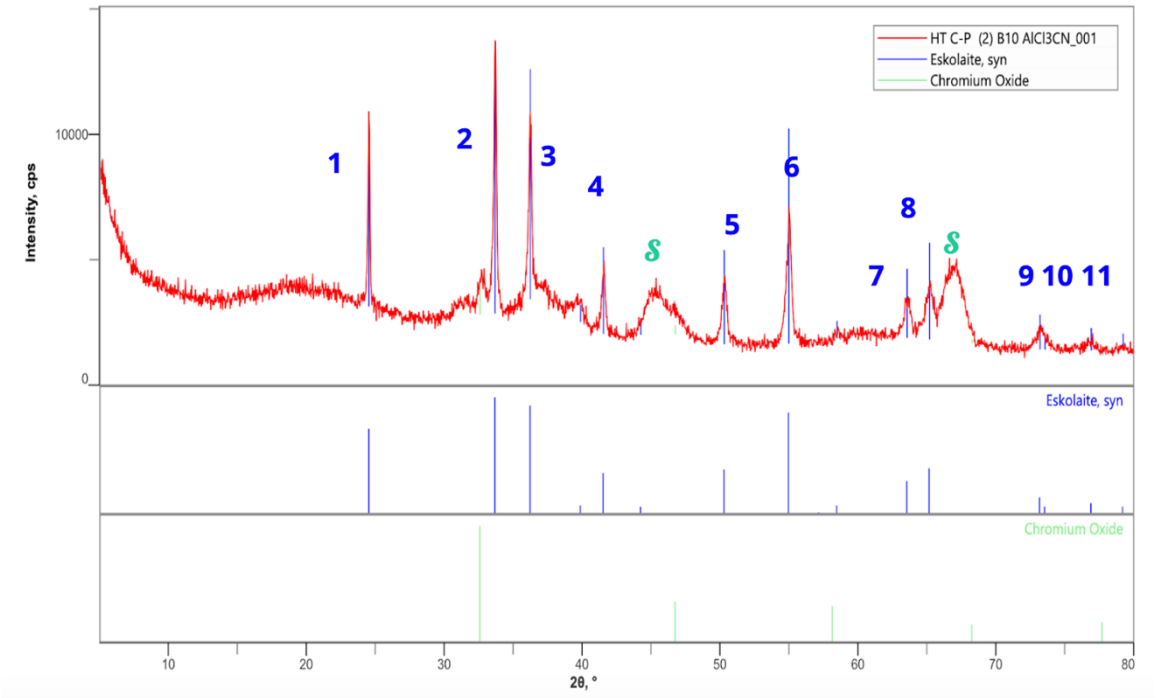

Figure 3-12: XRD pattern of chromia-alumina aerogel sample post-calcination. The matching software identified peaks due to eskolaite (blue), which is the mineral name for Cr_2O_3 and chromium oxide, Cr_2O_3 (green). The peaks labeled 1-11 match peaks correspond to α- Cr_2O_3. The two broad peaks labeled with the green "S" correspond to stainless steel, presumably due to contamination from the mold.

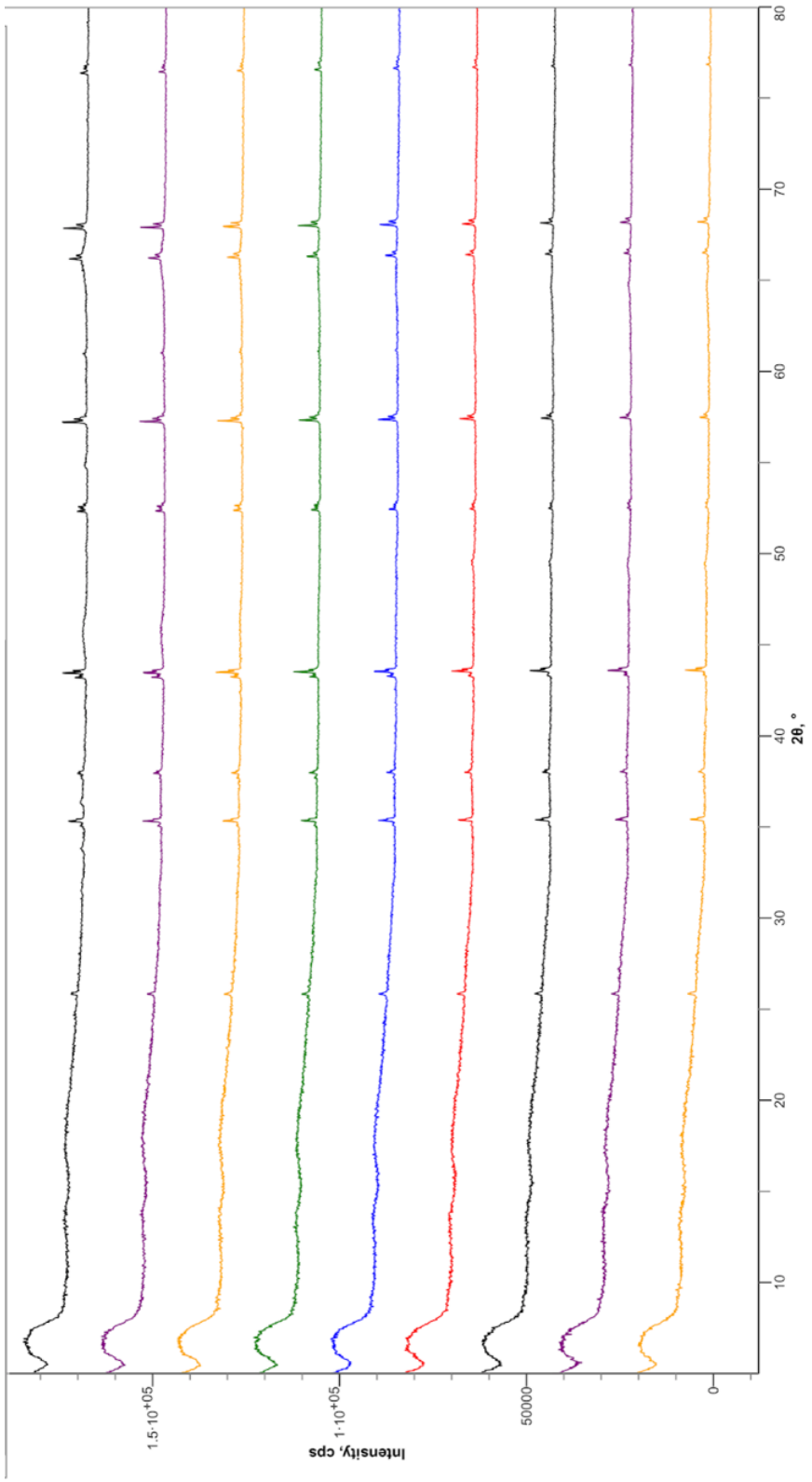

Figure 3-13: XRD analysis of as-prepared chromia-alumina aerogels using the furnace. From bottom (yellow peaks) to top (black peaks) the peaks present are for patterns obtained at: 26 °C, 100 °C, 200 °C, 300 °C, 400 °C, 500 °C, 600 °C, 700 °C, and 800 °C.

Surface Area Analysis

Surface area analyses were performed as-prepared and post-calcination to determine the overall surface area and pore volume of aerogel samples. Analysis of as-prepared aerogels resulted in BET surface areas of 700 ± 50 m^2/g (B4)[1] and 530 ± 30 m^2/g (B10). A plot of the pore volume vs. pore width for an as-prepared sample is depicted in Figure 3-14.

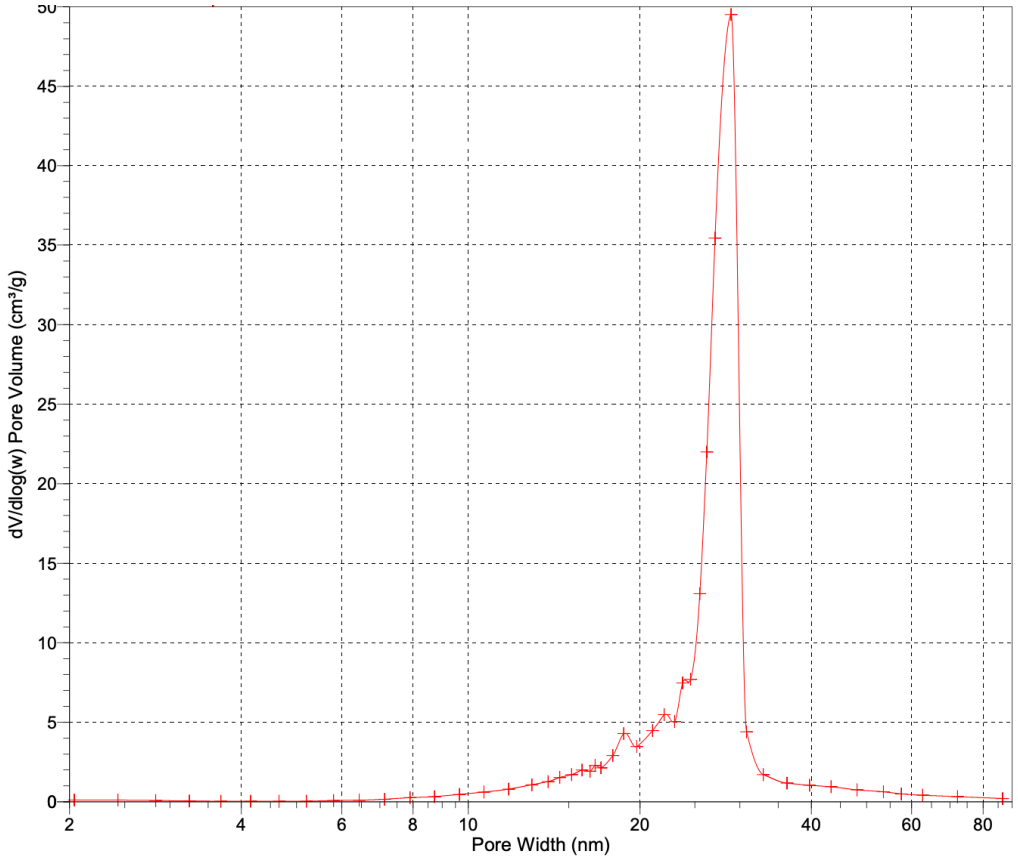

Figure 3-14: Pore volume of as-prepared aerogels (B4) as determined by the Micromeritics ASAP 2020 Surface Area and Porosity Analyzer. The calculated pore volume is 4.4 cm^3/g and average pore width is 23.5 nm (desorption).

[1] B4 nomenclature indicates "Batch 4." Batches were assigned numbers in sequential order based on the day they were produced. The same nomenclature was followed when labeling B10 and B15.

Surface area analysis of aerogels post-calcination resulted in average BET surface areas of 200 ± 10 m^2/g (B4) and 150 ± 8 m^2/g (B10). A plot of the pore volume vs. pore width for these samples is depicted in Figure 3-15.

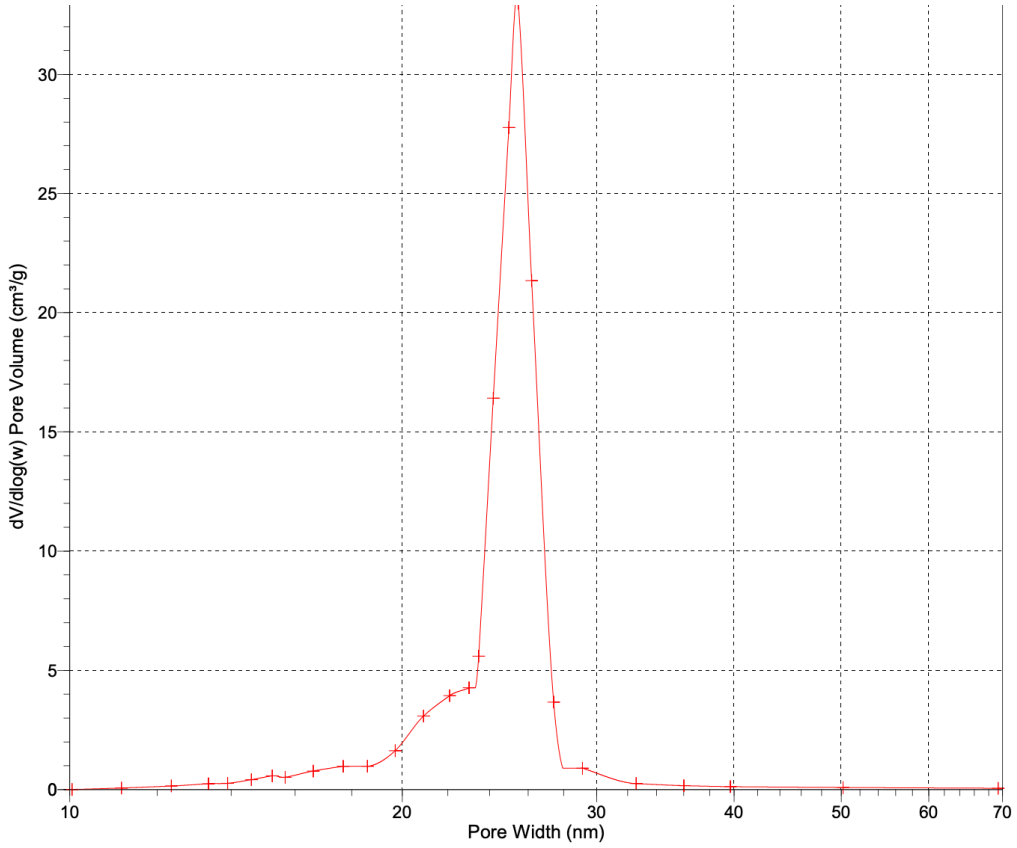

Figure 3-15: Pore volume of post-calcination aerogels (B4) as determined by the Micromeritics ASAP 2020 Surface Area and Porosity Analyzer. The calculated pore volume is 1.75 cm^3/g and the average pore width is 24.1 nm (desorption).

SEM/EDS Imaging

SEM imaging was employed to determine the topography of aerogel samples. EDS was also used to see the distribution of elements and dispersion of nanoparticles within the amorphous aerogel structure. Figure 3-16 depicts SEM and EDS images of chromia-alumina aerogels as-prepared. Figure 3-17 depicts SEM and EDS images of chromia-alumina aerogels post-calcination.

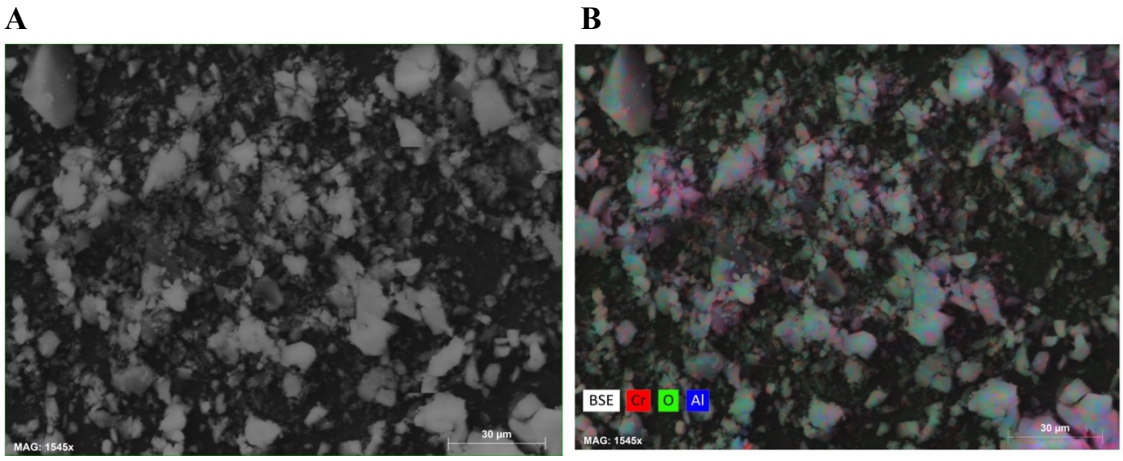

Figure 3-16: SEM image (**A**) and EDS image (**B**) taken at the same location and same magnification (note 30-µm scale bar) of as-prepared chromia-alumina aerogel samples. **B** shows the dispersion of Cr, O and Al throughout the aerogel.

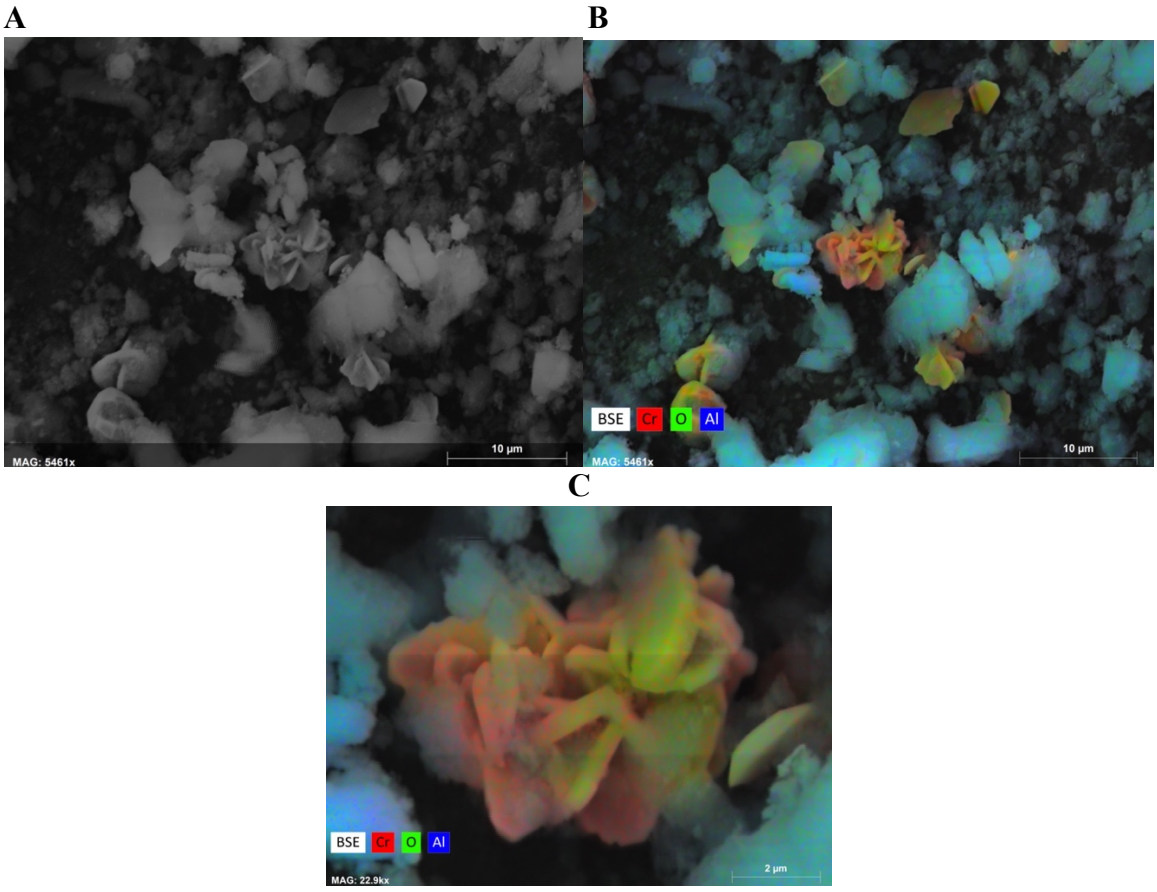

Figure 3-17: SEM image (**A**) and EDS image (**B**) taken at the same location and same scale (10 µm) of calcined chromia-alumina aerogel samples. **B** shows amorphous regions containing O and Al and microcrystals containing Cr and O. **C** depicts a better view of the chromia microcrystal (2 µm scale), the size of the nanocrystal aggregation is estimated to be about 8 µm in diameter.

Catalytic Testing

Four catalytic tests were performed on a 40-mL sample of calcined chromia-alumina aerogel in the Union Catalytic Testbed (UCAT). The conversion of the CO, propene (representing unburned hydrocarbons) and NO was measured using a five-gas analyzer, which detects these gases along with CO_2 and O_2. Results of conversion of CO, propene (hydrocarbons) and NO can be seen in Figures 3-18 through 3-20, respectively. Figure 3-21 presents the average conversion of CO, HC and NO under both high-air and low-air conditions.

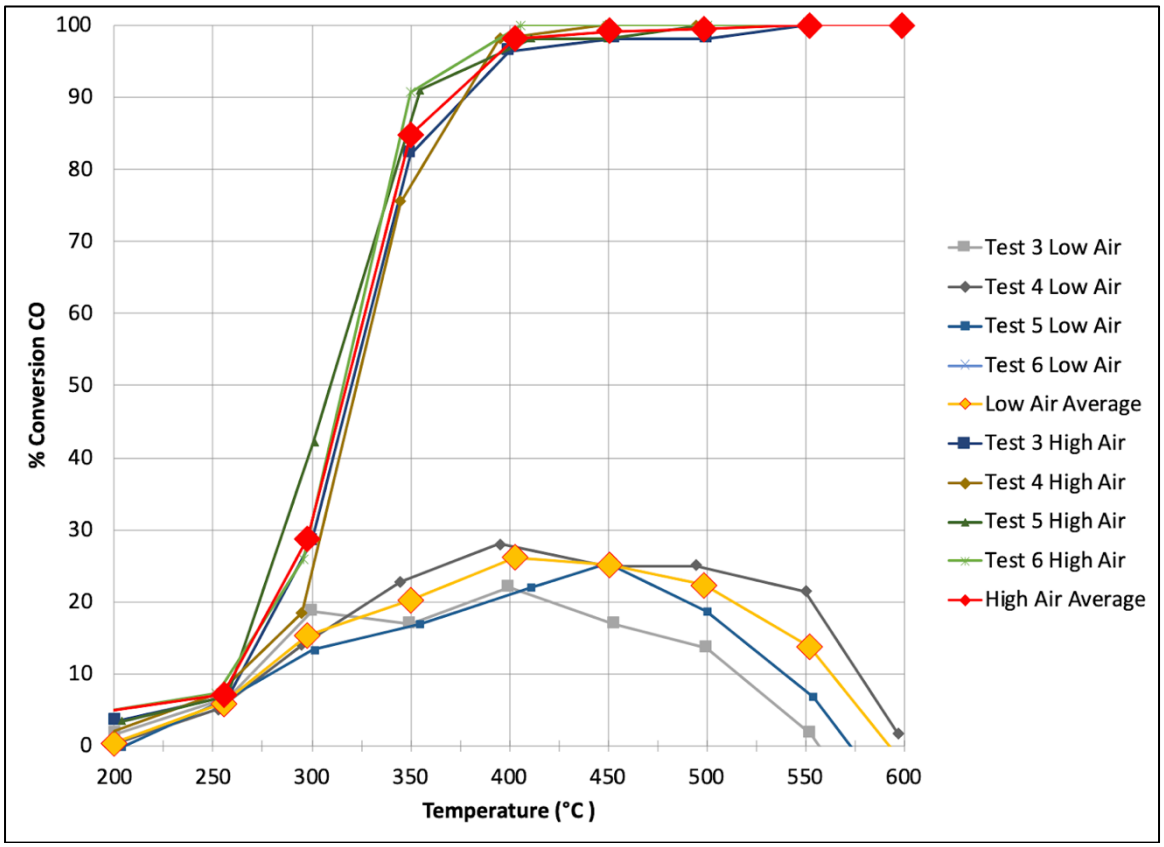

Figure 3-18: Percent conversion of CO by chromia-alumina aerogels under high-air and low-air conditions as a function of temperature. Lines are provided as guides for the eye.

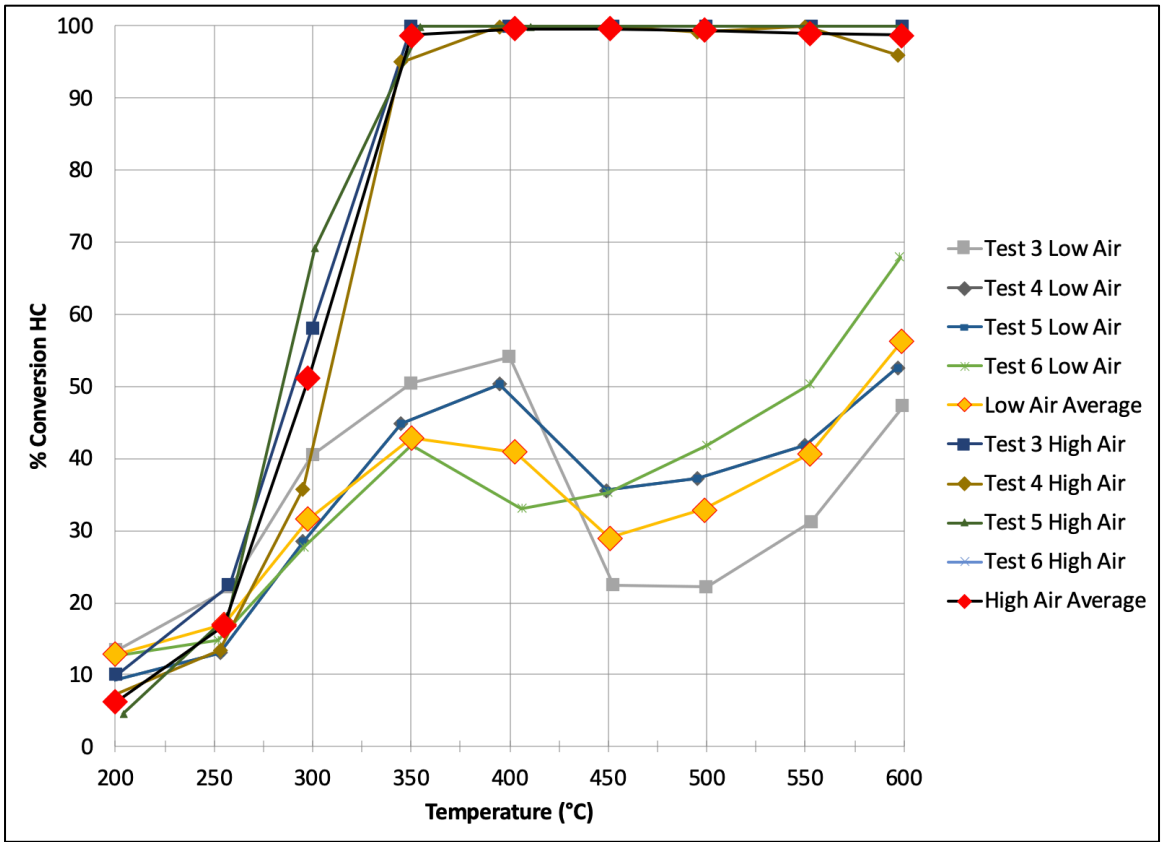

Figure 3-19: Percent conversion of HC (propene) by chromia-alumina aerogels under high-air and low-air conditions as a function of temperature. Lines are provided as guides for the eye.

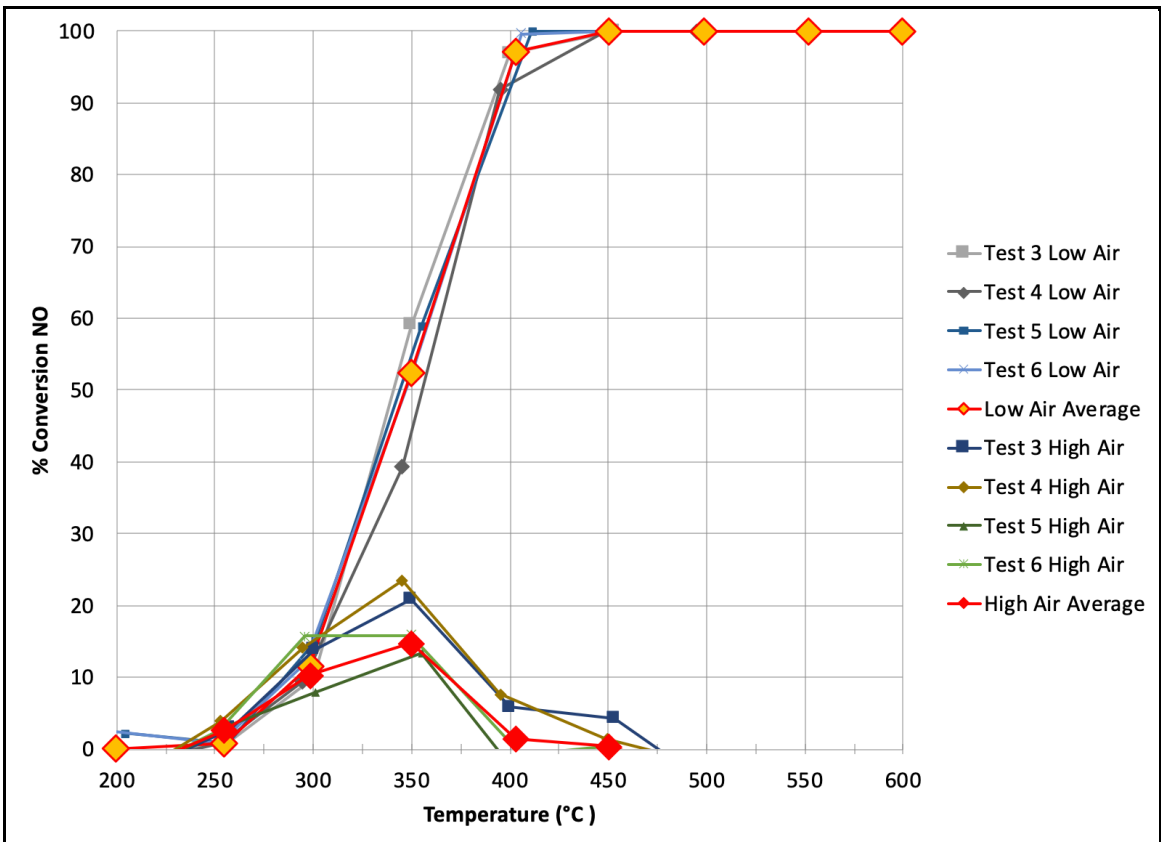

Figure 3-20: Percent conversion of NO by chromia-alumina aerogels under high-air and low-air conditions as a function of temperature. Lines are provided as guides for the eye.

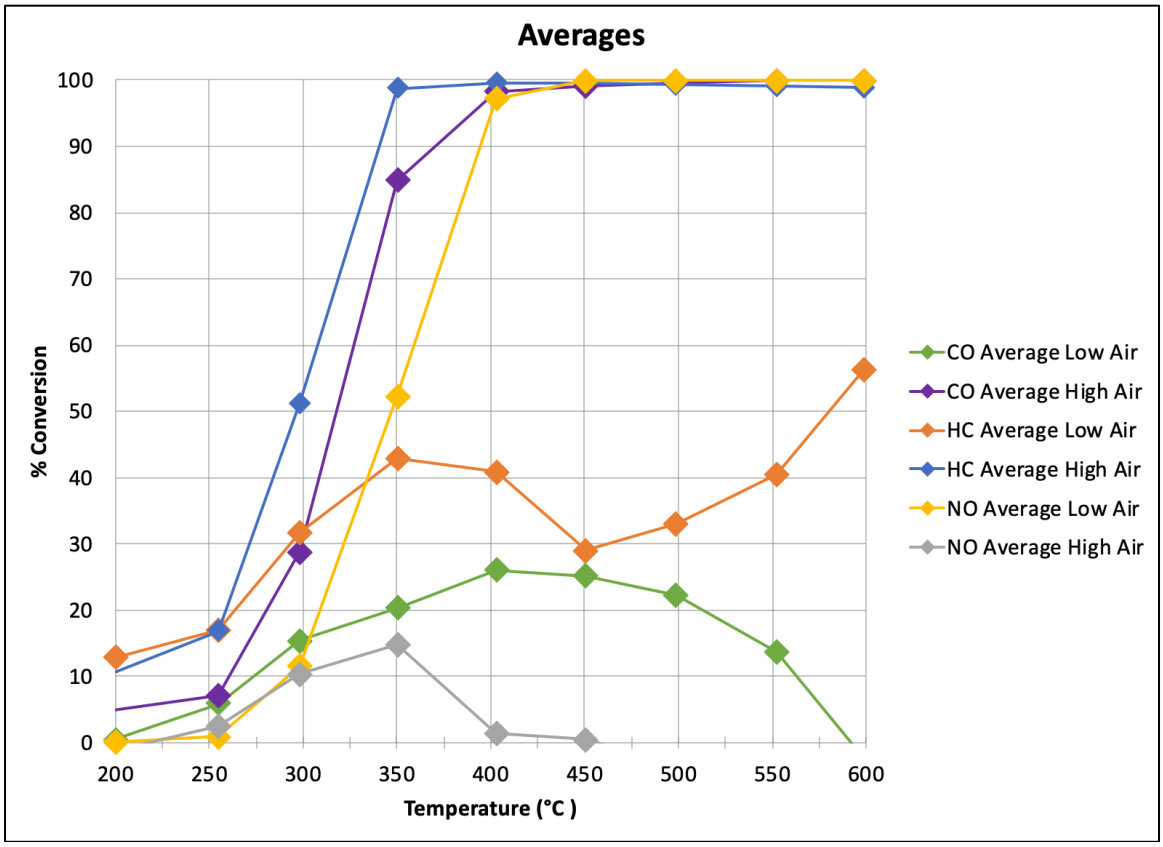

Figure 3-21: The average performance of chromia-alumina aerogel conversion of HC, NO and CO under high-air and low-air conditions. Lines are provided as guides for the eye.

Average percent conversion of each respective gas with calculated standard deviations can be seen in Table 3-1 for high-air conditions and Table 3-2 for low-air conditions. Note: in these tables the uncertainties reported are ± one standard deviation for the four replicate measurements. The temperature values (T) is also the average temperature across the four tests. Table 3-3 presents the average light-off temperature and percent conversion at 400 °C for each gas (CO, HC, NO) under high-air and low-air conditions.

Table 3-1: Average conversion of stimulated automotive exhaust by calcined chromia-alumina aerogels under high-air conditions

	Average Percent Conversion, High Air Condition					
Average T (°C)	CO	±	HC	±	NO	±
160	3	1	6	3	-4	1
255	7	0	17	4	3	1
298	30	10	50	10	10	4
350	85	8	99	3	15	5
403	98	2	100	3	1	6
451	99	1	100	1	0	3
499	100	1	99	1	-4	3
552	100	0	99	2	-8	5
599	100	0	99	2	-9	3

Table 3-2: Average conversion of simulated emissions by calcined chromia-alumina aerogel under low air conditions

	Average Percent Conversion, Low Air Condition					
Average T (°C)	CO	±	HC	±	NO	±
200	0	1	13	3	0	3
255	6	1	17	4	1	0
298	16	2	32	6	12	3
350	20	4	43	7	52	9
403	26	5	40	10	97	4
451	25	7	29	8	100	0
499	22	8	33	9	100	0
552	10	10	41	8	100	0
599	-2	15	56	9	100	0

Table 3-3: Light-off temperature and lowest temperature at which optimal conversion is reached under high-air and low-air conditions

	Low Air		High Air	
	Light off T (°C)	% conversion @ 400 °C	Light off T (°C)	% conversion @ 400 °C
HC	N/A	40 ± 14	300	100 ± 1
CO	N/A	26 ± 4	325	98 ± 2
NOx	350	97 ± 4	N/A	1 ± 6

4. DISCUSSION

Wet Gel Fabrication

The co-precursor technique resulted in a viable product, whereas the impregnation synthesis technique did not. Synthesis of chromia-alumina wet gels using the co-precursor technique was successful. Gelation occurred within 20 minutes of the addition of propylene oxide. A chromia-alumina wet gel with a 5:1 mole ratio of alumina salt to chromium salt has a characteristic non-translucent dark midnight-blue color (Fig 3-3).

The physical characteristics of the chromium salt solution and chromia-alumina wet gel agreed with observations of chromia-based aerogels from Kucheyev et al., in which their chromium solution (chromium(III) chloride hexahydrate) was characterized by a translucent dark-blue color and their wet gel was characterized by a blue/green color [1]. The forest-green color sometimes seen in chromium-aluminum salt solutions or with addition of propylene oxide is most likely due to the ligation of chromium(III). Chromium(III) acts as an acid (with H_2O ligands) and is usually a "violet-blue-grey" color, but when a hydroxide ion is lost to a basic solution (the dissociation of the H_2O ligand) the result is a green solution [2]. Green chromium(III) solutions are also known to form when the ligand is chloride or excessive hydroxide ions are added to solution [3]. It can be concluded that the dissociation of the H_2O ligands on chromium(III) or the presence of chloride from the aluminum salt solution caused the solution mixture to change from a dark-blue color to green (Fig 3-2).

Solvent Exchanges

48 hours was the selected time interval to perform solvent exchanges because when they were performed every 24 hours, the aerogels produced through RSCE were inconsistent. The "inconsistent" chromia-alumina aerogels did not possess the physical characteristics of aerogels and looked more like xerogels. They were described as "burnt and collapsed."

No loss of chromium salt was noted during solvent exchanges. The solvent poured off the wet gel during each solvent exchange was nearly colorless, as presented in Figures 3-3 through 3-5.

Rapid Supercritical Extraction

Significant shrinkage occurs during the RSCE processing of chromia-alumina wet gels. The 87% shrinkage of chromia-alumina aerogels is larger than shrinkage seen through RSCE production of other catalytic aerogels containing Ce, Co, Cu, Ni and V [4, 5, 6, 7, 8]. The reason for the shrinkage seen in chromia-alumina aerogels with processing is, at present, unknown. Literature reports of chromia aerogels doped with platinum or gold, indicate that shrinkage of the pores was seen during the drying step due to capillary forces [9]. Even though the RSCE process is supposed to preserve the structure of the pores of the sample while extracting the solvent (absolute ethanol) above its supercritical point the addition of metal compounds can cause additional stress. In the present work, the observed shrinkage was consistent across all co-precursor chromia-alumina aerogels produced via RSCE.

Chromia-alumina aerogels produced through RSCE in Mold 1 are characterized by a deep-green color and sometimes are coated in a light-green powder, as depicted in

Figure 3-7. When aerogels are processed in the hydraulic hot press using the Mold 2 (Figure 2-2), the color of the as-prepared aerogels is slightly different (Figure 3-8). They are a blue-green color with a brown dusting coating the aerogel pieces. However, characterization of B15 (in which half the batch was processed through the hot press in Mold 1 and the remaining half in Mold 2) via XRD and SEM/EDS confirmed there are no obvious chemical differences between the as-prepared aerogels produced in the two different molds.

Aerogel Calcination

Heat treatment of as-prepared chromia-alumina aerogel samples caused further shrinkage, on average an additional 55% volume was lost. However, the mass of the materials changed less drastically through calcination, which accounts for the ~50% increase in density seen between the as-prepared samples (0.21 ± 0.03 g/mL) and post-calcination samples (0.30 ± 0.02 g/mL). The calculated density of as-prepared chromia-alumina aerogels agrees with the literature value of about 0.2 g/mL of as-prepared chromia-aerogel monoliths [1].

Differences in color of post-calcination chromia-alumina aerogels (noted in Figure 3-10) appear to be related to the mold employed for RSCE processing, which is an unexpected result. Mold 1 and Mold 2 have wells of different volumes. Characterization of both post-calcined samples confirmed there are no apparent chemical differences between the post-calcination aerogels that were processed through the hydraulic hot press in the two different molds.

XRD

XRD analysis of as-prepared and post-calcination chromia-alumina aerogels gives insight into the structures and phases of crystalline components of the materials, specifically chromium oxides. Figure 3-11 presents peak analysis of as-prepared chromia-alumina aerogels, in which the intensities of the observed peaks are quite low and, in many cases, not visible due to background noise. However, Figure 3-11 verifies that as-prepared aerogels contain a mixture of Cr^{3+} and Cr^{4+} which are the two oxidation states of chromium present in Cr_3O_8. The as-prepared chromia-alumina aerogels primarily amorphous but contain microcrystals. This is supported by the literature which states that Cr4+ is most commonly seen in amorphous chromium while Cr3+ is found in the crystal field [1]. The "corundum" (Al_2O_3) peaks in Figure 3-11 match peaks in Figure 3a of a publication by Boumaza et al., which correspond to α-alumina [10]. Post-calcination chromia-alumina aerogels (Fig. 3-12) possess peaks of stronger intensity that correspond to eskolaite, Cr_2O_3. Peaks 1 through 11 in Figure 3-12 correspond to peaks observed for chromia catalysts Cr-1 and Cr-3 in Rotter et al., 2003 [11]. Eskolaite, the mineral name for α-Cr_2O_3, is the most common phase of chromia observed in other applications of bulk chromia catalyst [1, 11]. Chromia eskolaite corresponds to the hexagonal, α-Cr_2O_3 crystalline structure of chromia in which the oxidation state is Cr^{3+} [11].

Surface Area Analysis

The total BET (Brunauer-Emmett-Teller) surface area of as-prepared chromia-alumina aerogels (Table 4-1, B4 and B10) decreases by about 75% after calcination (Table 4-1, B4 HT and B10 HT). The BJH (Barrett-Joyner-Halenda desorption) average

pore volume decreases by about 50% upon calcination. These data, along with the 55% decrease in volume verifies further shrinkage of materials occurs during the 24 hrs of calcination at 800 °C. However, a slight increase in average pore width is seen in post-calcined samples compared to as-prepared samples which could possibly be due to multiple small pores collapsing into fewer large pores. Surface area and structural data collected for chromia-alumina aerogels is compared to literature data for other chromia-based aerogels as well as other TMO catalytic aerogels fabricated using the Union College RSCE method in Table 4-1.

Table 4-1: Physical and structural properties of chromia-alumina aerogels compared to literature values

Aerogel Sample	BET Surface Area (m^2/g)	Pore Volume (cm^3/g)	Pore Diameter (nm)
B4	700 ± 50	4.4	25.1 *
B4 HT	200 ± 10	1.8	36.0 *
B10	530 ± 30	2.4	17.9 *
B10 HT	150 ± 8	1.2	32.0 *
Cr-3 [11]	110	0.1	5.1 *
Cr-7 [11]	630	0.8	5.3 *
CrOOH [13]	670	3.4	20
Alumina [12]	670 ± 20		37
CeAl (CP) [4]	114 ± 6		
CoAl [5]	700 ± 30		
CuAl-B [6]	430 ± 30		
V-Al [7]	500 ± 40		
Ni(10%)Al [8]	750 ± 30		20 ± 2

* indicates that pore diameter was calculated using a formula adapted from Rotter et al., 2003 [11].: d = 4 x (pore vol/SA) x 1000.

As-prepared RSCE chromia-alumina aerogels (B4, B10) have surface areas comparable to other aerogels prepared by the Union College RSCE, specifically alumina aerogels, cobalt-alumina aerogels (CoAl) and 10% nickel-alumina aerogels (Ni(10%)Al). As-prepared RSCE chromia-alumina aerogels can be compared to Cr-7 and CrOOH aerogels described in Rotter et al. [11, 13]; these materials are all characterized by an amorphous structure. As-prepared RSCE chromia-alumina aerogels (B4, B10) possess surface area and pore characteristics similar to the literature values, [11, 13].

The decrease in surface area seen between as-prepared chromia-alumina aerogels (B4, B10) and post-calcination chromia-alumina aerogels (B4 HT, B10 HT) is comparable to the difference in surface area between Cr-7 and Cr-3 respectively [11]. As-prepared chromia-alumina aerogels and post-calcination chromia-alumina aerogels were compared to aerogel samples Cr-7 and Cr-3 [11] respectively due to similar fabrication processes and physical structures. Cr-7 aerogels are characterized by their amorphous structure and were prepared by ambient temperature aging and dried by supercritical flow of CO_2, similar to as-prepared chromia-alumina aerogels. Cr-3 aerogels are characterized by the presence of α-Cr_2O_3 and were prepared by precipitation with ammonium hydroxide and calcination, similar to the post-calcined chromia-alumina aerogels [11].

SEM/EDS

SEM and EDS results give insight into the chemical composition of nanoparticles observed within the aerogel structure. EDS photos of as-prepared chromia-alumina aerogels (Figure 3-16B) show chromium, oxygen and aluminum particles evenly dispersed in the nanomaterial, which confirms that as-prepared chromia-alumina aerogels are largely amorphous. However, post-calcination chromia-alumina aerogels (Figure 3-

17B) show clusters of chromium and oxygen (chromia) nanocrystals dispersed throughout the aluminum- and oxygen-containing (alumina) backbone, which agrees with the XRD data of post-calcined aerogels. A conclusion can be made that post-calcination chromia-alumina aerogels are mostly amorphous with deposits of chromia (α- Cr_2O_3) nanocrystals throughout the material.

Catalytic Testing

UCAT testing confirms that calcined chromia-alumina aerogels act as three-way catalysts and efficiently convert carbon monoxide (CO), propene (HC) and nitric oxide (NO). Chromia-alumina aerogels with the high-air gas formulation flow, which most closely mimics oxidizing conditions, efficiently and fully convert CO and HC to less noxious gases. The light-off temperature of CO conversion occurs at 325 °C and 100% conversion is reached and maintained at about 400 °C. The light-off temperature of HC conversion occurs at 300 °C and 100% conversion is reached and maintained by 400 °C. CO and HC conversion under low-air conditions present inconsistent data, characterized by spikes and dips seen in the conversion data. Less than 50% conversion is seen under these conditions, which means the light-off temperature was not reached. This confirms that high-air (1.15% O_2, oxidative conditions) is necessary in order to convert carbon monoxide and hydrocarbons to less noxious gases. This is verified by the poor conversion of CO and HC under low-air conditions (0.12% O_2), in which minimal oxygen is present.

Nitric oxide (NO) is best converted under low-air conditions which correspond to the optimal conditions for reduction reactions. Under low-air conditions the light-off temperature occurs at 350 °C and about 100% conversion is reached and maintained by 450 °C. The reduction of NO under high-air conditions is inconsistent due to the negative

conversion values seen at high temperatures. Negative conversion values seen from 500 °C - 600 °C are due to the gas analyzer measuring more NO than was initially flowed through (> 1130 ppm, Table 2-10). The "higher" NO detection could be due to a number of reasons such as: the concentration of the two values of NO gas which are being measured are the same within the uncertainty in the measurement (so there is no conversion), the detector (five-gas analyzer) is at its limit, or there is a possibility that more NO is actually being produced.

Copper-alumina (CuAl) aerogels are one of the most promising TMO aerogel TWC produced in our laboratory. Tobin et al., fabricated CuAl aerogels composed of 14% Cu (w/w) which efficiently converted CO and HC under high air conditions and NO under low air conditions [6]. However, the gas mixture used in these experiments was "BAR97 low emission blend" so these results cannot be directly compared to the CLEERS Dry Gas mixture used in the chromia-alumina studies (Table 2-10). Control catalytic testing was performed with "4-g" CuAl aerogels using the CLEERS Dry Gas mixture to ensure conversion using a new gas mixture was similar to the conversion described by Tobin et al. [6]. Data collected from UCAT testing of the control 4-g CuAl sample are presented in Table 4-2.

Table 4-2: Average light-off temperature and percent conversion at 400 °C for each gas (CO, HC, NO) under high-air and low-air conditions with 4-g CuAl aerogels.

	Low Air		**High Air**	
	Light off T (°C)	% conversion @ 400 °C	Light off T (°C)	% conversion @ 400 °C
HC	N/A	30 ± 20	275	99 ± 2
CO	N/A	30 ± 20	275	98 ± 2
NOx	375	70 ± 40	N/A	9 ± 1

Under high-air conditions when converting HC and CO, 4-g CuAl aerogels reach their light-off temperature at a lower temperature (275 °C) than chromia-alumina (CrAl) aerogels (HC 300 °C, CO 325 °C). Complete (100%) conversion of HC is reached at a lower temperature as seen CrAl aerogels compared to CuAl aerogels; however, the opposite is seen for 100% conversion of CO. Under low-air conditions, CrAl aerogels reach the light-off temperature at a lower temperature than CuAl aerogels and also reach 100% conversion before CuAl aerogels. These data demonstrate that chromia-alumina aerogels have significant promise for TWC applications compared to other TMO aerogel catalyst.

Discussion References

[1] Kucheyev, S. O.; Sadigh, B.; Baumann, T. F.; Wang, Y. M.; Felter, T. E.; Buuren, T. V.; Gash, A. E.; Satcher, J. H.; Hamza, A. V. Electronic Structure of Chromia Aerogels fromSoft x-Ray Absorption Spectroscopy. *Journal of Applied Physics* **2007**, *101*(12).

[2] Lennartson, A. The Colours of Chromium. Nature Chemistry 2014, 6 (10), 942–942.

[3] Clark, J. Chromium. https://www.chemguide.co.uk/inorganic/transition/chromium.html (accessed Apr 28, 2020).

[4] Posada, L. F.; Carroll, M. K.; Anderson, A. M.; Bruno, B. A. Inclusion of Ceria in Alumina- and Silica-Based Aerogels for Catalytic Applications. *The Journal of Supercritical Fluids* **2019**, *152*, 104536.

[5] Bouck, R. M.; Anderson, A. M.; Prasad, C.; Hagerman, M. E.; Carroll, M. K. Cobalt-Alumina Sol Gels: Effects of Heat Treatment on Structure and Catalytic Ability. *Journal of Non-Crystalline Solids* **2016**, *453*, 94–102.

[6] Tobin, Z. M.; Posada, L. F.; Bechu, A. M.; Carroll, M. K.; Bouck, R. M.; Anderson, A. M.; Bruno, B. A. Preparation and Characterization of Copper-Containing Alumina and Silica Aerogels for Catalytic Applications. *Journal of Sol-Gel Science and Technology* **2017**, *84*(3), 432–445.

[7] Smith, L. C.; Anderson, A. M.; Carroll, M. K. Preparation of Vanadia-Containing Aerogels by Rapid Supercritical Extraction for Applications in Catalysis. *Journal of Sol-Gel Science and Technology* **2015**, *77*(1), 160–171.

[8] Bruno, B. A.; Madero, J. E.; Juhl, S. J.; Rodriguez, J.; Dunn, N. J. H.; Carroll, M. K.; Anderson, A. M. "Alumina-Based Aerogels as Three-Way Catalysts." Conference proceedings of the Ninth International Congress on Catalysis and Automotive Pollution Control (CAPoC9), August 2012.

[9] Rotter, H.; Landau, M. V.; Herskowitz, M. Combustion of Chlorinated VOC on Nanostructured Chromia Aerogel as Catalyst and Catalyst Support. *Environmental Science & Technology* **2005**, *39*(17), 6845–6850.

[10] Boumaza, A., Favaro, L Lédion, J, Sattonnay, J. Brubach, P, Berthet, A, Huntz, P, & Tétot, R. "Transition Alumina Phases Induced by Heat Treatment of Boehmite: An X-ray Diffraction and Infrared Spectroscopy Study." Journal of Solid State Chemistry 182 (2009): 1171-1176.

[11] Rotter, H.; Landau, M.; Carrera, M.; Goldfarb, D.; Herskowitz, M. High Surface Area Chromia Aerogel Efficient Catalyst and Catalyst Support for Ethylacetate Combustion. *Applied Catalysis B: Environmental* **2003**, *47*(2), 111–126.

[12] Juhl, S. J.; Dunn, N. J.; Carroll, M. K.; Anderson, A. M.; Bruno, B. A.; Madero, J. E.; Bono, M. S. Epoxide-Assisted Alumina Aerogels by Rapid Supercritical Extraction. *Journal of Non-Crystalline Solids* **2015**, *426*, 141–149.

[13] Landau, M. V.; Shter, G. E.; Titelman, L.; Gelman, V.; Rotter, H.; Grader, G. S.; Herskowitz, M. Alumina Foam Coated with Nanostructured Chromia Aerogel: Efficient Catalytic Material for Complete Combustion of Chlorinated VOC. *Industrial & Engineering Chemistry Research* **2006**, *45*(22), 7462–7469.

5. CONCLUSIONS AND FUTURE WORK

Conclusions

Chromia-alumina aerogels were successfully fabricated using the co-precursor technique and a 5:1 mole ratio of aluminum salt to chromium salt. Minimal shrinkage was seen in the formation of the wet gel and no chromium was lost throughout the solvent exchanges (Fig. 3-4A). Chromia-alumina aerogels were created using the RSCE technique via the hydraulic hot press. However, 87% shrinkage was seen with processing through the hydraulic hot press and additional 55% shrinkage was seen with calcination. Change in color, volume, density and other physical characteristics were observed and noted with calcination of all chromia-alumina aerogel batches fabricated.

XRD analysis along with SEM/EDS images of the chromia-alumina aerogels as-prepared and post-calcination verify that as-prepared aerogels have an amorphous structure (Fig. 3-11 and Fig. 3-16) while physical and structural changes occur in the aerogels with calcination due to the presence of α-Cr_2O_3 nanocrystals dispersed in the alumina backbone (Fig. 3-12 and Fig. 3-17). Structural changes in the chromia-alumina aerogels are also verified with the changes in BET surface area, BJH pore volume and pore diameter seen between as-prepared aerogels and post-calcination aerogels (Fig. 3-14, Fig. 3-15, Table 4-1).

Preliminary catalytic tests show that chromia-alumina aerogels are promising TWCs. Chromia-alumina aerogels efficiently convert carbon monoxide and hydrocarbons under high-air (oxidative) conditions and convert nitric oxide under low-air (reducing) conditions (Table 3-3).

Future Work

Future work on catalytic chromia-based aerogel project will be focused on increasing production, characterization and catalytic testing of the aerogels. Many of these studies would have been performed and included in this thesis if not for the move to online classes during the Spring of 2020 due to the Covid-19 pandemic. Future work includes the following studies:

1. Chromium loading experiments using the co-precursor synthesis technique. Preliminary experiments were performed, in which chromia-alumina aerogels were fabricated with salt molar ratios of 10:1 aluminum chloride hexahydrate:chromium nitrate nonahydrate and 2.5:1 aluminum salt:chromium salt. Only fabrication and preliminary XRD studies of chromia-alumina aerogels has been performed as depicted in Figure 5-1; no other characterization techniques have been used to study chromia-alumina aerogels of different doses.

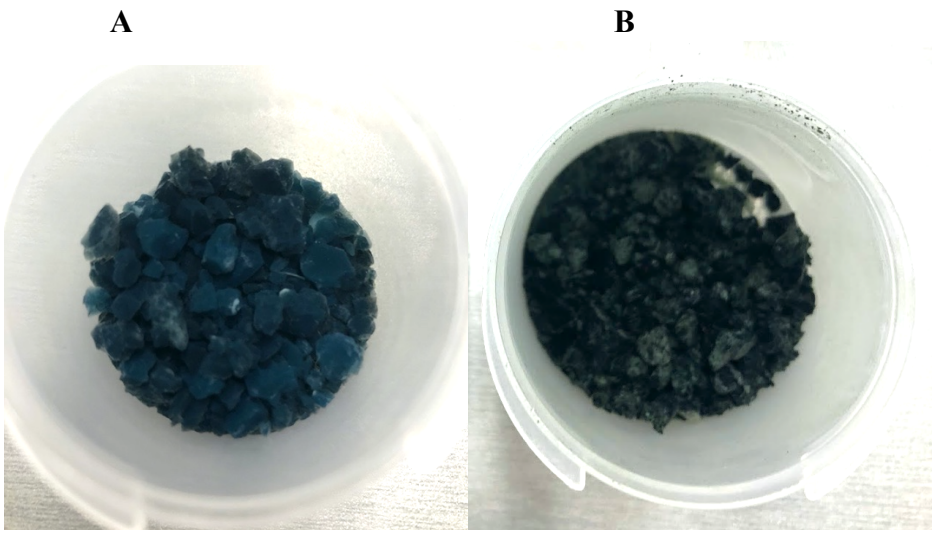

Figure 5-1: A depicts as-prepared chromia-alumina aerogels prepared from a 10:1 aluminum:chromium salt precursor mixture. **B** depicts aerogels formed from a 2.5:1 aluminum:chromium salt precursor.

2. Fabricate chromia-alumina aerogels via the impregnation technique as described by Juhl et al. [1] and Posada et al. [2]. Preliminary experiments in this thesis resulted in poor wet gel formation, while preliminary practicum work conducted by Margeaux Capron shows a viable chromia-alumina aerogel product via the impregnation technique.

3. Investigate alternate gelation methods, such as ammonium hydroxide. Ammonium hydroxide has successfully been used to induce gelation in silica aerogels and is less toxic, volatile and carcinogenic than propylene oxide [3]. The literature also explains physical changes (such as color and precipitate formation) associated with reactions of chromium (III) and ammonia [4].

4. Characterization via IR spectroscopy must be performed to understand the type of bonds in chromia-alumina aerogels.

5. Shrinkage studies must be conducted to understand why drastic shrinkage is seen with fabrication and calcination of chromia-alumina aerogels. The RSCE processing is supposed to mitigate shrinkage [5] and shrinkage on this scale has not been seen with production of other TMO catalytic aerogels (Ce, Co, Cu, Ni and V) [2, 6, 7, 8, 9].

Conclusions and Future Work References

[1] Juhl, S. J.; Dunn, N. J.; Carroll, M. K.; Anderson, A. M.; Bruno, B. A.; Madero, J. E.; Bono, M. S. Epoxide-Assisted Alumina Aerogels by Rapid Supercritical Extraction. *Journal of Non-Crystalline Solids* **2015**, *426*, 141–149.

[2] Posada, L. F.; Carroll, M. K.; Anderson, A. M.; Bruno, B. A. Inclusion of Ceria in Alumina- and Silica-Based Aerogels for Catalytic Applications. *The Journal of Supercritical Fluids* **2019**, *152*, 104536.

[3] Durães, L.; Oliveira, O.; Benedini, L.; Costa, B. F.; Beja, A. M.; Portugal, A. Sol–Gel Synthesis of Iron(III) Oxyhydroxide Nanostructured Monoliths Using $Fe(NO_3)_3 \cdot 9H_2O/CH_3CH_2OH/NH_4OH$ Ternary System. *Journal of Physics and Chemistry of Solids* **2011**, *72*(6), 678–684.

[4] Clark, J. Chromium. https://www.chemguide.co.uk/inorganic/transition/chromium.html (accessed Apr 28, 2020).

[5] Bono, M. S.; Anderson, A. M.; Carroll, M. K. Alumina Aerogels Prepared via Rapid Supercritical Extraction. *Journal of Sol-Gel Science and Technology* **2009**, 53(2), 216–226.

[6] Bouck, R. M.; Anderson, A. M.; Prasad, C.; Hagerman, M. E.; Carroll, M. K. Cobalt-Alumina Sol Gels: Effects of Heat Treatment on Structure and Catalytic Ability. *Journal of Non-Crystalline Solids* **2016**, *453*, 94–102.

[7] Tobin, Z. M.; Posada, L. F.; Bechu, A. M.; Carroll, M. K.; Bouck, R. M.; Anderson, A. M.; Bruno, B. A. Preparation and Characterization of Copper-Containing Alumina and Silica Aerogels for Catalytic Applications. *Journal of Sol-Gel Science and Technology* **2017**, *84*(3), 432–445.

[8] Smith, L. C.; Anderson, A. M.; Carroll, M. K. Preparation of Vanadia-Containing Aerogels by Rapid Supercritical Extraction for Applications in Catalysis. *Journal of Sol-Gel Science and Technology* **2015**, *77*(1), 160–171.

[9] Bruno, B. A.; Madero, J. E.; Juhl, S. J.; Rodriguez, J.; Dunn, N. J. H.; Carroll, M. K.; Anderson, A. M. "Alumina-Based Aerogels as Three-Way Catalysts." Conference proceedings of the Ninth International Congress on Catalysis and Automotive Pollution Control (CAPoC9), August 2012.